A Comprehensive Review of DC–DC Converter Topologies and Modulation Strategies with Recent Advances in Solar Photovoltaic Systems

Kummara Venkat Guru Raghavendra [1], Kamran Zeb [1,2], Anand Muthusamy [1], T. N. V. Krishna [1], S. V. S. V Prabhudeva Kumar [1], Do-Hyun Kim [1], Min-Soo Kim [1], Hwan-Gyu Cho [1,*] and Hee-Je Kim [1,*]

[1] School of Electrical Engineering, Pusan National University, Busandaehak-ro 63beon-Gil, Geumjeong-gu, Busan 46241, Korea; kvg.raghavendra999@gmail.com (K.V.G.R.); kami_zeb@yahoo.com (K.Z.); anand.muthusamy07@gmail.com (A.M.); vamsik.tirumalasetty@gmail.com (T.N.V.K.); vasavisai9999@gmail.com (S.V.S.V.P.K.); kdh8486@naver.com (D.-H.K.); rlaalstn5122@naver.com (M.-S.K.)

[2] School of Electrical Engineering and Computer Science, National University of Sciences and Technology, Islamabad 44000, Pakistan

* Correspondence: hgcho@pusan.ac.kr (H.-G.C.); heeje@pusan.ac.kr (H.-J.K); Tel.: +82-51-510-2364 (H.-J.K); Fax: +82-51-513-0212 (H.-J.K)

Abstract: Renewable Energy Sources (RES) showed enormous growth in the last few years. In comparison with the other RES, solar power has become the most feasible source because of its unique properties such as clean, noiseless, eco-friendly nature, etc. During the extraction of electric power, the DC–DC converters were given the prominent interest because of their extensive use in various applications. Photovoltaic (PV) systems generally suffer from less energy conversion efficiency along with improper stability and intermittent properties. Hence, there is a necessity of the Maximum power point tracking (MPPT) algorithm to ensure the maximum power available that can be harnessed from the solar PV. In this paper, the most important features of the DC/DC converters along with the MPPT techniques are reviewed and analyzed. A detailed comprehensive analysis is made on different converter topologies of both non-isolated and isolated DC/DC converters. Then, the modulation strategies, comparative performance evaluation are addressed systematically. At the end, recent advances and future trends are described briefly and considered for the next-generation converter's design and applications. This review work will provide a useful structure and reference point on the DC/DC converters for researchers and designers working in the field of solar PV applications.

Keywords: DC/DC converter; control; MPPT; photovoltaic (PV) systems; modulation strategies

1. Introduction

The economic progress of any country majorly relies on the energy that can be regarded as the key input for the development. The rapid growth of industries, vehicles and domestic users led to the consumption of the energy on a large scale. The fossil fuels are depleting day by day and the pollution caused to the atmosphere, an increase of the global temperature are considered to be the dominant challenges to protect the environment. Hence there is a need to rely on renewable energy sources to produce electrical energy. Among all Renewable Energy Sources (RES) the Photovoltaic (PV) power generation has become significant because of its unique merits such as longer lifespan, eco-friendly, mobile and portability of various parts, the capability of the output power to meet the peak loads [1].

Solar power tracking has become a great issue because of the nonlinear behavior in the PV panel's current-voltage (I–V) characteristics that are operated employing a maximum power point (MPP) [2].

Since the power delivered by the PV panel depends on the atmospheric conditions generally referred to as the solar irradiance and accessible temperature of the cell. These parameters are not consistent and vary according to the atmospheric conditions. Hence it is necessary to employ maximum power point trackers [MPPT] [3]. MPPT is a critical component in the solar PV system to draw the maximum power. Furthermore, the converter employed with an MPPT achieves the load matching and delivers the maximum power [4].

The main factor affecting solar PV systems is the abnormal availability of solar irradiances. To overcome this problem and to supply a constant output voltage, various power electronic DC–DC converters are used. Since the 1920s, the DC–DC converter was established to be employed with solar PV units. The main purpose of the power electronic converters was to replace the use of the conventional circuits such as rheostat and potential dividers often referred to as simple voltage divider circuits. The drawback of this technique is that the output voltage obtained is less in comparison with the input voltage resulting in reduced efficiency [5].

These days, there are various DC–DC converter topologies that are employed to regulate the input voltage suitable to the application's requirements as shown in Figure 1. The basic classification of the DC–DC converters is into two types, such as the isolated DC–DC converter and the non-isolated DC–DC converter. In the construction of the isolated DC–DC converters, there is an electrical barrier created by using a high-frequency transformer in between the input and outputs of the converter. This phenomenon is used to protect the sensitive loads, the output of the converter can be configured with positive or negative polarity and it has very high noise interference capability [6].
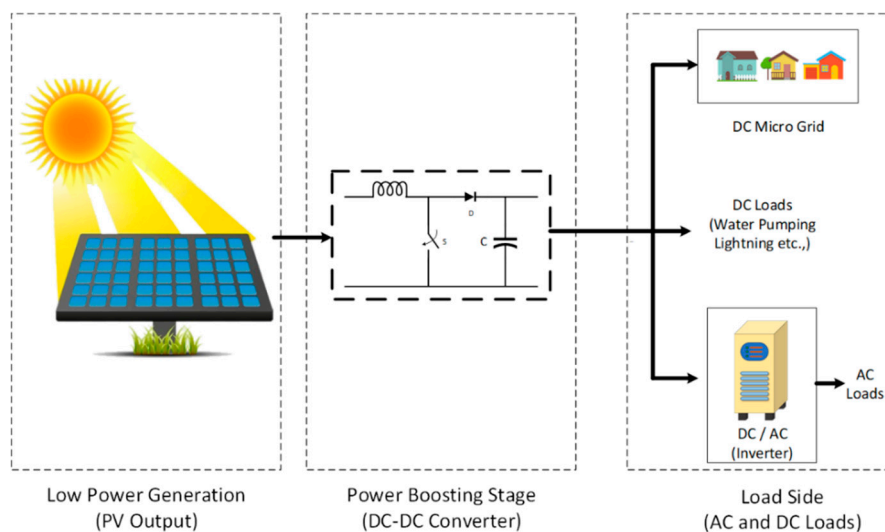
Figure 1. Solar PV integrated system with DC–DC converters fed to the load [2,6].

In the case of non-isolated DC–DC converters, the electrical barrier supposed to be absent and this enables the non-isolated converters to have a simple design and to cost less. In the literature, a prominent number of non-isolated converters are studied. There are several DC–DC converter topologies that were developed pertaining to the greater efficiencies, switching and control strategies, fault-tolerant configurations and widely on the renewable energy-based applications [7–17].

This review article is arranged as follows. In Section 1, the introductory part is explained that gives an idea about the importance of renewable energy sources. This section is followed by Section 2 the discussion of annual global PV demand and its future forecast was illustrated. Furthermore, in Sections 3 and 4, various power electronic non-isolated and isolated converters that were employed to achieve optimum performance in the solar PV application system are explained. In Section 5, a concise review of the MPPT techniques is made and Section 6 illustrates the modulation strategies of various converters with the recent literature. This section is followed by Section 7, where the comparative performance of various converters was demonstrated. Sections 8 and 9 reveals some

interesting recent advancements in the DC–DC converters and draws conclusions from the review study. Table 1 clearly summarizes the contribution of the proposed review article along with the various surveys that were already published and mentioned in the literature.

Table 1. Comparative analysis of various surveys on converters and control schemes.

| References	GPV	CT	MS	MPPTT	CA	RA	M	DM	EA	Focused Area
[18]	x	✓	x	✓	✓	x	✓	✓	x	Solar PV systems
[19]	x	✓	x	x	✓	✓	x	✓	x	Renewable Energies
[20]	x	✓	x	x	✓	x	x	x	x	Renewable Energies
[21]	x	✓	x	x	✓	x	x	x	✓	Distributed generation units
[22]	x	✓	x	x	✓	✓	x	x	✓	Renewable energy and energy storage systems
[23]	x	✓	x	x	✓	x	✓	✓	✓	PV applications
[24]	x	✓	x	✓	✓	✓	x	x	✓	DC Microgrids
[25]	x	✓	x	✓	✓	x	✓	✓	✓	Solar PV systems
[26]	x	✓	x	✓	✓	x	✓	✓	x	Solar PV systems
[27]	x	✓	✓	✓	✓	✓	x	x	x	PV, wind, HVDC Applications
[28]	x	✓	x	x	✓	x	✓	✓	✓	Solar PV systems
This work	✓	✓	✓	✓	✓	✓	✓	✓	✓	Solar PV systems

Note: GPV-Global PV Status; CT-Converter Topologies; MS-Modulation strategies; MPPTT-Maximum PowerPoint Tracking Techniques; CA-Comparative Assessments; RA-Recent Advances; M-Merits; DM-Demerits; EA-Elemental Analysis.

2. Global PV Market

Many countries around the world are now are looking at the installation of PV power plants and the number of power plants increased considerably, which resulted in an increased proportion of alternative energy sources for the generation of electricity [29]. The electrical energy production by PV increased from 3.7 to 7 GW between 2004 and 2007. From 2008 to 2011, it increased from 7 to 40 GW. In one decade, 2004–2014, the PV share increased from 3.7 to 177 GW [30,31]. In 2016, the cumulative global PV capacity was found to be 303 GW. The global trend in the advancement of installed PV capacity can be observed in Figure 2a [32], and Figure 2b depicts the actuals and the forecast of both the wind and solar energy sources [33].

From the beginning, as shown in Figure 2b, wind generation took a dominant position, of 17 GW over solar PV generation that was just found to be 1.3 GW in the year 2000. Until 2018, the trend continued. A recent report pertaining to the wind and solar energies found that they reciprocate each other, showing that there is a potential dependency on solar-based generation. Nearly 789 GW of energy demand fell on solar PV systems, where it was 722 GW for on wind generating units. The report forecasted that by 2023 the solar PV generation systems will drastically increase to 1296 GW when it is 903 for wind generation units.

The rapid increase in the global PV demand is the result of demand for electricity, the need to reduce the emission of carbon dioxide, more advances in the potentials of solar PV's and the efficient operation of the solar PV in integration with the electric grid.
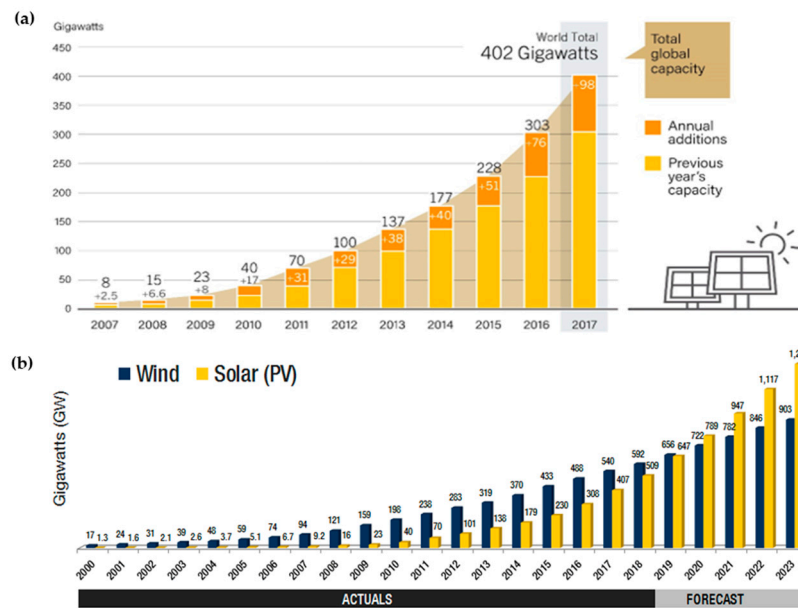
Figure 2. (**a**) Installed global solar photovoltaic (PV) capacity (2007 to 2017) [31]. (**b**) The actuals and the forecast of both the wind and solar energy sources [32].

3. Classification of the DC–DC Converters

The era of the power converters created a dramatic shift in the evolution of the various advancements in the electrical field. Moreover, conventional power converters always hold a dominant position for their applications and unique characteristics. The following section will evaluate the classification of the converters and their application in the PV system applications.

Basically, DC–DC converters are categorized into isolated and non-isolated converters as shown in Figure 3. The isolation alludes the presence of an electrical barrier in between the inputs and outputs of the converter. A high-frequency transformer can act as this barrier. The main advantage of this barrier is to be employed for the high voltage applications. Furthermore, these isolated converters can either be configured as positive or negative. This barrier is absent in non-isolated converters. Fly back, forward, resonant, push-pull, bridge converters come under the isolated converters. Cuk, SEPIC, boost, buck–boost, positive-output super-lift Luo and Ultra-lift Luo converters are the non-isolated converters that are majorly employed.
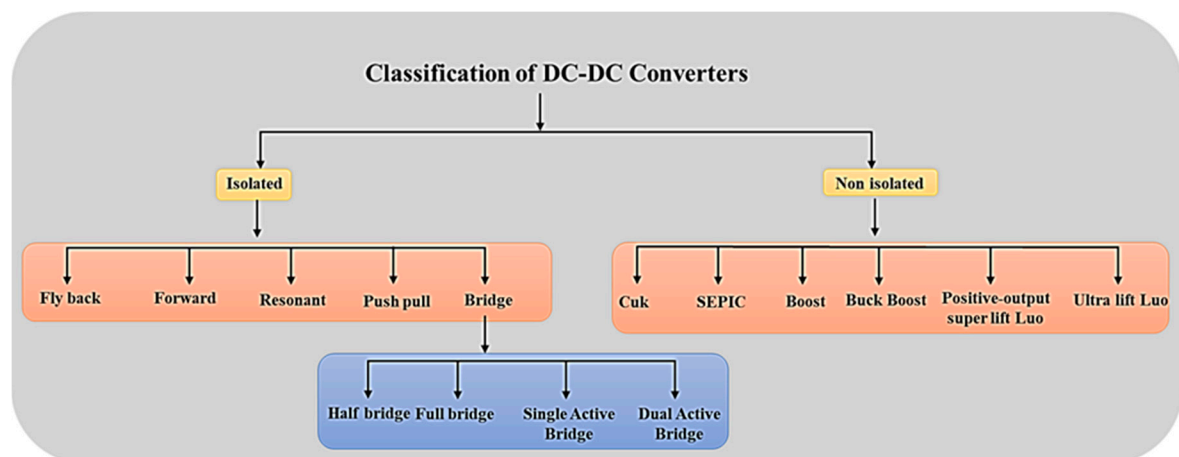
Figure 3. Classification of DC–DC converters for Solar PV applications.

3.1. Buck Converter

The DC–DC buck converter, shown in Figure 4, steps down the output voltage level to be less when compared with the input voltage level [34,35]. Therefore, this converter topology can be employed for integrating the greater module voltages to the lower loads or lower battery voltages. There are various solar PV applications used along with the DC–DC buck converters, are employed in the standalone solar PV pumping systems that are enabled to use the water supply in rural areas [36], solar battery charger [37,38], grid-connected MPPT tracking [39], and the off-grid PV systems [40].
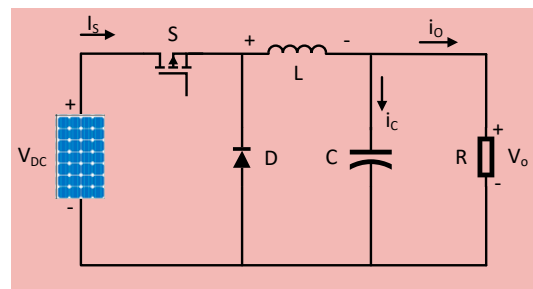

Figure 4. Buck converter for the PV application [34].

3.2. Boost Converter

In certain PV applications, the load side voltage magnitude needs to be a greater value in comparison the output voltage. In that case, the boost converter is employed in the MPPT converter. There are many modifications and much research that was proposed by researchers to enhance the performance of the boost converters (Figure 5) [41–43].

Huber and Jovanovic et al. [44] used the cascade structure to minimize the ripples and increase the voltage gain. Since the input voltage is less, it is found that the initial cascaded structure has to be less voltage stress that can operate with enhanced with the switching frequencies. Furthermore, the second part operated with less switching frequency, thereby curtailing the switching losses. The main drawback of the cascaded structure was the circuit with the greater number of components, less efficiency and the noise affected by Electromagnetic interference (EMI).

The coupled inductor and a switched capacitor are used to enhance the voltage gain of the boost converter. When compared to the two separate inductors, one coupled inductor can use the magnetic core effectively and therefore it reduces the magnetic loss and the ripple content. The main usage of the leakage inductance of the coupled inductor enables diminishing the reverse recovery problems at the output side [45]. Moreover, the enhanced switching loss and current stress are the major flaws. The clamp circuit is employed to decrease the voltage spikes that occur at switches of the MOSFET [46].
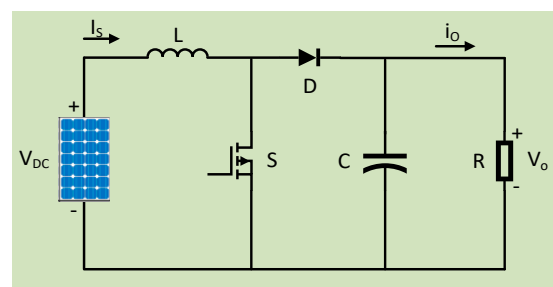

Figure 5. Boost Converter for PV Application [42].

3.3. Buck–Boost Converter

The buck–boost converter in Figure 6 is formed by integrating basic buck and boost converter topology and that can be used in various applications as standalone/grid-connected PV systems and

motor drives [47]. The current research on the buck–boost converter is still under progress for solar PV applications [48–54]. To enhance the voltage gain, many researchers across the world are developing various non-isolated DC–DC converter topologies namely Cuk, SEPIC, and Luo converters that are constructed relying on the buck–boost topology.

When the buck–boost converters are operated in the continuous conduction mode (CCM), the ripples in the currents are shown to be less. In comparison with the single switch buck–boost converters, two switch buck–boost converters said to have minimum voltage and current stress on operating components. Ahmed et al. [55] discussed that a two-switch buck–boost converter operated non-inverting can store the current additionally. Perturb and Observe MPPT algorithm-based technique is used to get optimal MPPT operation. Furthermore, the experimental results also depicted that the designed converter has greater efficiency when operated with the dominant heavy load applications. The proposed converter can operate in two modes such as PWM-controlled mode buck or boost usually depends on the condition of the instantaneous input voltage corresponding to the output voltage.
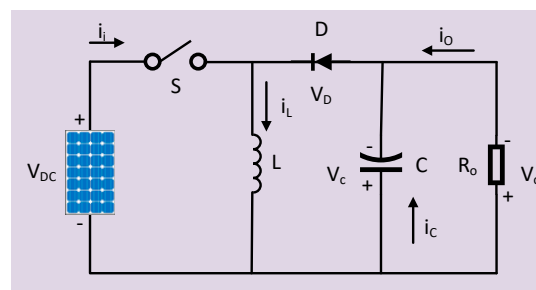

Figure 6. Buck–Boost converter for PV application [48].

3.4. Single-Ended Primary Inductance Converter (SEPIC)

The single-ended primary inductance converter is shown in Figure 7 and generally refered as a SEPIC converter. Basically, during switching, the ON time is more than the OFF time to achieve the output voltage higher (because of more time of charging for the inductor). If not, the converter ceases to provide the required output. This is because the capacitor cannot fully charge.

There are several constraints that need to be considered during the designing of the converter. When a high-frequency transformer is operated with the conventional SEPIC converter, the ripple in the output voltage is supposed to reduce. This setup benefits with the key features like output current to be continuous, minimizing the switching stress, and output ripple [56–59]. During AC–DC conversion, certain harmonics were induced, that lead to the ripples in AC currents, eventually resulting in reducing the power factor.

When the SEPIC converter operates in the boundary conduction mode (BCM), this converter can be used for power factor correction in AC lines [60]. Pertaining to the solar power generation, the SEPIC can be widely implemented to control DC voltage flickerings. To enhance the robustness, there are various control methodologies implemented such as PI control, sliding mode control, dP/dV feedback control, fuzzy logic control is recommendable to attain the maximum power [61–63]. The SEPIC converter is implemented for sensorless control of a solar-fed DC motor that can extend its application to solar-based transportation [64]. Soft switching is used to diminish the losses during the design of the converter, which can be further used in minimizing the output current ripples [65,66].
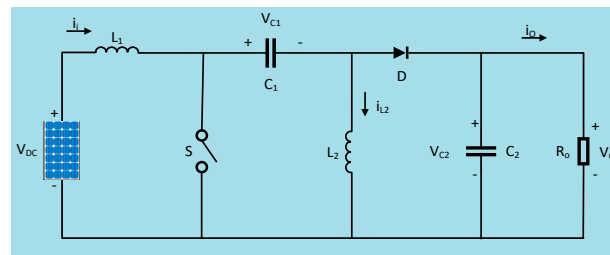
Figure 7. SEPIC converter for the PV application [56].

3.5. Cuk Converter

The basic constructional feature of the Cuk converter, as shown in Figure 8, can be better understood from the basic buck–boost converter that was replaced with the capacitor instead of the inductor used for storage of the energy and the power transfer. Also, the fly back DC–DC converter with the negative-output capacitive energy [66]. The output voltage polarity of the cuk converter is supposed to be reversed corresponding to the input voltage. With suitable connections, the output of the converter is inverted resulting in the ripple-free output which further can be used for various kind of applications [67–70].

In the literature [71–76], various conventional cuk converters are presented. The overall efficiency of the modified cuk converters is recommendable for an optimal bidirectional operation that aims to regulate the voltage and current's [77]. In the closed-loop system, there are various techniques such as proportional-integral (PI) and the sliding mode control that can be incorporated with the fuzzy logic controller to control the output voltage [78,79]. Despite this, the Cuk converter can be employed in the BLDC motor drive circuit [66] and renewable energy applications such as the PWM-based photovoltaic system [80–85].
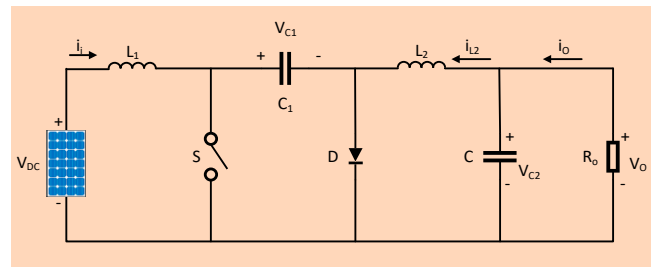

Figure 8. Cuk converter for PV application [72].

3.6. Positive-Output Super-Lift Luo Converter

Super-lift Luo converters, shown in Figure 9, are very powerful when compared to the cuk and the SEPIC converters. The unique features of this converters are its enhanced efficiency, the output voltage generated in terms of the arithmetic progression. When considering the positive-output super-lift Luo converters, these converters possess higher transfer voltage gain if they are operated in the first quadrant. Moreover, these types of converters are still under research for their application in domestic and industries [86–89].

Initially, Luo et al. [90] introduced this super-lift technique that was incorporated with the series energy storage elements such as a series capacitors and series inductors that are responsible for the greater voltages in the output resembling the higher geometric progression and Yefim Berkovich et al. [91] made some modifications in the positive-output super-lift Luo converter that possess higher voltage transfer gain. Furthermore, Kumar et al. [92] used the sliding mode controller operated in the parallel positive-output elementary super lift Luo converter in order to balance the proper sharing of the load current and the voltage regulation.
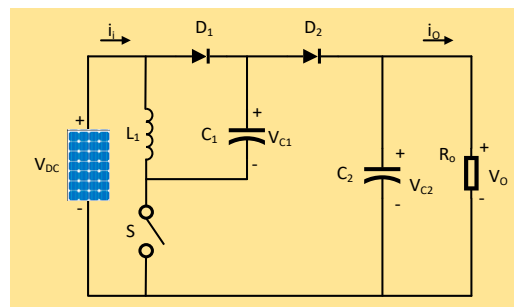
Figure 9. Positive output super-lift Luo converter for PV application [87].

3.7. Ultra-Lift Luo Converter

Ultra-lift Luo converters, shown in Figure 10, exhibit the much higher values of the conversion of voltage transfer gain at the output. The voltage transfer gain obtained by this converter is the product of the voltage lift Luo converter and the super-lift Luo converter [93]. The design of the closed-loop controller is tedious since the output voltage is assumed to be the highest value with small variations obtained in the duty ratio. The efficiency of this converter is presumed to be the highest value among all other non-isolated DC converters [94].
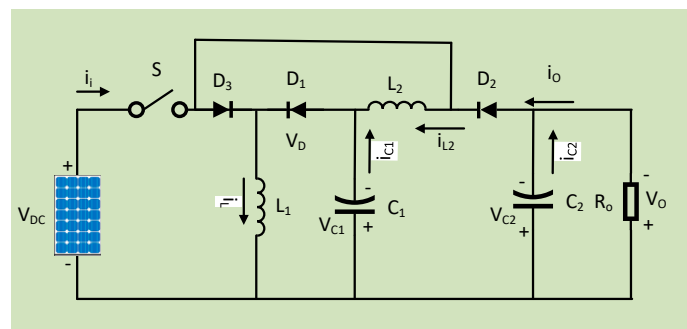
Figure 10. Ultra-lift Luo converter [93].

3.8. Zeta Converter

Zeta converter, shown in Figure 11, delivers a non-inverted voltage at the output that is either enhanced or diminished value when compared to the input voltage, such as the SEPIC converter [95–101]. The two important features of the zeta converters are, for example, the buck–boost, Cuk, and SEPIC converters. The important feature of the Zeta converter operated in the solar PV panel is that it is enabled to track MPP over the entire area of the PV curve. Antonio et al. [102] illustrated a new kind of Zeta converter that is constituted with the boost converter used for the battery storage ability in the PV system applications. The proposed topology shown some good parameters such as reduced input and output current ripple, enhanced voltage conversion ratio and operated well in both the CCM and the DCM modes.

Figure 11. Zeta converter for PV application [97].

4. Isolated DC–DC Converter Topologies

4.1. Flyback Converter

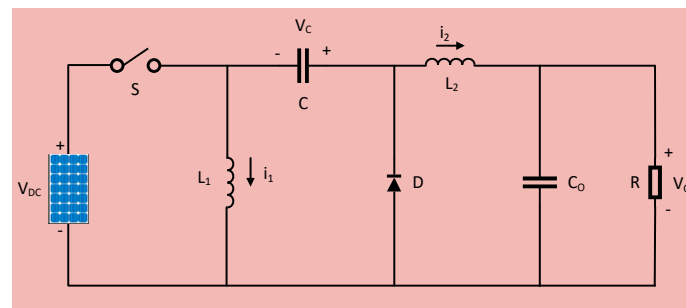The flyback converters, shown in Figure 12, are mainly employed in the solar PV system applications of the ultra-low power. Whenever there is a requirement of converter gain to be higher, along with employing the transformers, the key solution is the usage of the flyback converters. For high power applications, the transformer needs to have a large air gap to store energy. The large airgap is responsible for the less magnetizing inductance, flyback converters deliver a greater leakage flux and very less efficiency of energy transfer. Although the cuk converters are used in the applications of high power, they have certain drawbacks such as polarity inversion of the output and higher flow of current in the powered switch and the diode at the output [103]. Lu et al. [104] implemented an isolated grid-connected inverter that had been integrated with the interleaved flyback converter topology that was operating in the DCM model. Therefore this converter showed some unique features, such asswift dynamic response and the system also seemed less complex. Furthermore, the efficiency of the flyback converters can be enhanced by the ZVS operation [105]. Soft switching is obtained by employing the clamp circuits along with the resonant-based flyback converters. Achille et al. [106] implemented a soft switching dual flyback converter and achieved a decreased ripple content and obtained the higher efficiencies [107].
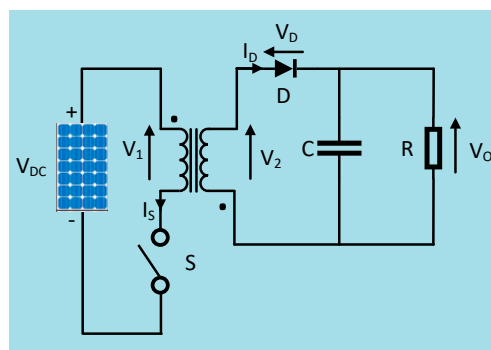
Figure 12. Flyback converter for PV application [105].

4.2. Bridge Converter

The bridge converter is one of the kinds of DC–DC converter topologies employing four or two active switching components in a bridge configuration across high-frequency power transformer.

4.2.1. Half-Bridge Converter

A three port half-bridge converter was designed for renewable energy system applications, as shown in Figure 13. The primary circuit of the half-bridge converter is functioned as a synchronous rectification-buck converter and allowing the DC bias current into the high-frequency transformer. A post-regulation and synchronous regulations with various implementations are projected. It achieves independent regulation on three ports with the benefits of modest converter topology, simple control, and single-stage power conversion [108]. An active-clamped half-bridge DC converter with three switches were implemented. It achieves continuous input current with low ripple and wide range ZVS [109].
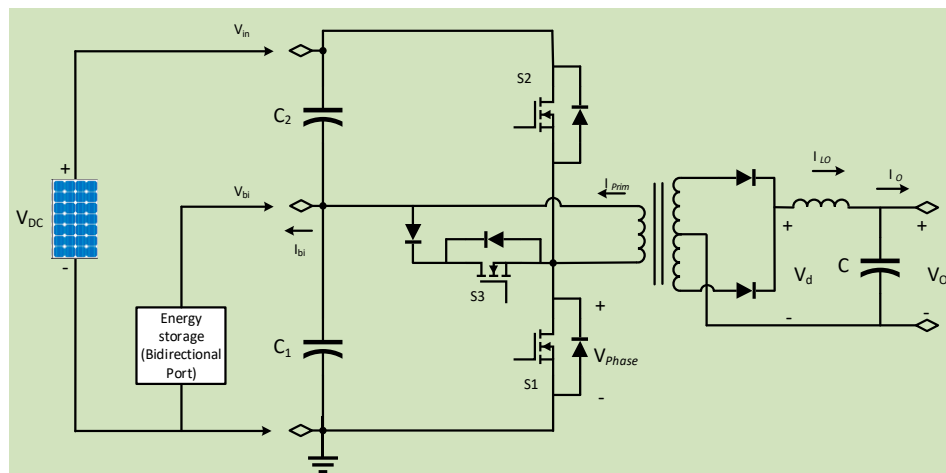
Figure 13. Three port half-bridge converter for PV application [108].

Dual half-bridge LLC resonant converter is proposed using a hybrid secondary rectifier used for wide input voltage applications. In this topology, the hybrid secondary rectifier can act as a voltage doubler rectifier or voltage quadruple rectifier depends on the switching strategy of the dual half-bride circuit. The proposed converter can yield high voltage gain along with a voltage quadruple rectifier [110]. High performance interleaved DC converter was employed explored to raise output power with high efficiency. In this topology a half-bridge work in a region to ensure the two interleaved duty cycle close to 50% which makes the continuous output current width without lag and reduces the component size [111]. High voltage bi-directional half-bride three-level converter was proposed in this manuscript for high voltage DC microgrid application. This topology can accomplish a high efficiency by reducing voltage stresses and electromagnetic interference [112].

4.2.2. Full-Bridge Converter

A full-bridge converter, as shown in Figure 14, is generally used in the renewable energy systems to interface the renewable source, storage device, and load. Full-bridge- three-port converter which integrates two buck–boost converters into the full-bridge topology. A single power conversion stage and zero voltage switching for all the available switches can be achieved at this topology easily [113]. A highly efficient asymmetrical pulse-width-modulated full-bridge converter was implemented for the renewable energy system applications. This converter designed with full-bride topology and asymmetric control scheme to obtain the zero voltage switching while turn-on the switches which minimize the circulating current loss. The resonant part of the circuit which combined with leakage inductance and blocking capacitor provides the zero current switching's while turn-off the switches. It eliminates the reverse recovery problem of the output diode. Overall the suggested Asymmetrical PWM full-bridge converter gain fewer stresses on power switches and achieved high efficiency [114]. Full-bridge CLL resonant topology with a capacitive output filter was implemented for achieving wider input voltages at the renewable energy system. It also obtains zero voltage switching and achieved high power conversion efficiency. These converters obtained high stability while varying the input voltage and output load in a wide range [115].
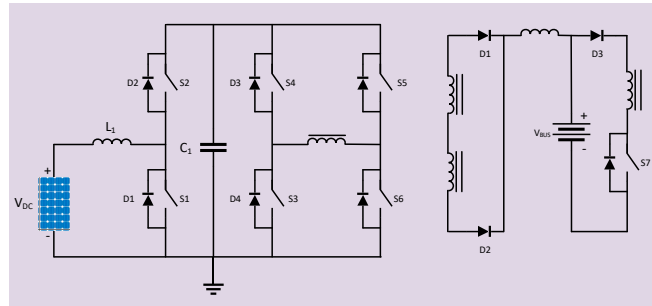
Figure 14. Full-bridge converter for PV application [113].

4.2.3. Dual Active Bridge Converter

The Dual Active Bridge – Isolated Bidirectional DC–DC Converter (DAB-IBDC) topology in Figure 15, is popular among the researchers due to its essential characteristics such as bidirectional power flow, high conversion efficiency, galvanic isolation, high power density, and inherent soft switching property. These features enable the DAB-IBDC an important circuit for standalone hybrid system application [116–118]. The two full bridges are isolated by using the high-frequency power transformer which leakage inductance that work as an energy storage element. The primary bridge is attached to high voltage DC source and the secondary bridge is connected to low voltage energy storage device or load. The square wave between both bridges can be conveniently phase shifted with respect to each other to enable the bidirectional power flow. The power conversion took place because of controlling the voltage difference across the energy storage element [119]. The future trends and the design considerations of the DAB converter and also the high-frequency DAB transformer was discussed briefly in the literature obtained from [120,121]. The performance of an ultra-capacitor-based DAB converter dynamic was modeled and presented [122]. The various digital control techniques and implementation method were analyzed for the DAB-IBDC converter [123,124].
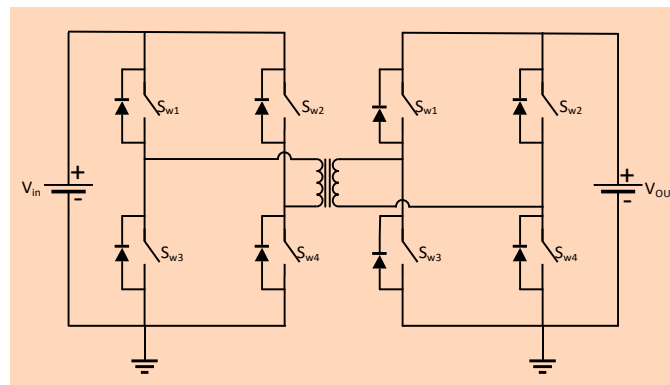
Figure 15. DAB converter for PV application [117].

4.2.4. Multi-Element Resonant Converter

The improved topology of the conventional LLC converter called a multi-element resonant converter in Figure 16a. It achieves high power density and higher efficiency at full load so that gaining much more attention in front end converters for renewable power systems and battery chargers for electric vehicles [125,126]. Both ZVS and ZCS operating conditions can be achieved in these converters using a short output circuit [127–129]. The multi-element resonant converter typically formed using five resonant components that connected serial or parallel in a circuit. A few of the multi-element connections are shown in Figure 16a. Based on this, two-element, three-element, and four-element resonant converters were designed. Because it consists of multiple resonant components, the multi-element

resonant converter experiences various resonant frequencies. Due to the suitable placement of existing frequencies, the transmission of the fundamental and the third-order harmonic active power is guaranteed.

(a) Three elements LLC resonant converter Figure 16b: The resonant tank was formed using three LLC element and it is considered to be a bandpass filter in a circuit which comprises parallel resonant frequency (PRF) and series resonant frequency (SRF) [130,131]. The series resonant frequency is created by the capacitor and inductor of the resonant tank. The fundamental component of input energy can be distributed form source to load very efficiently at this topology. Therefore, high power conversion efficiency can be achieved very easily using this topology. However, to achieve the proper damping effect, the frequency must be increased largely as it has poor frequency selectivity and very wide bandwidth. An additional resonant element must be added for improving the characteristics of this topology.

(b) Four-element resonant converter, as shown in Figure 16c: The LCLC four-element converter is 3-element LLC-based resonant topology [132,133]. The magnetic construction and resonant parameter design method for four-element topologies are simple in logic and accurate. It achieves high voltage gain and high conversion efficiency. This topology is particularly suitable for wide input voltage applications such as standalone energy system. It experiences optimum weighted efficiency over the extensive input voltage range.

(c) Five-element resonant converter, as shown in Figure 16d: The five-element LLC-LC resonant converter is implemented by adding two LC elements into the secondary side of the traditional conventional LLC converter [134]. The additional two LC elements called notch filter which increases the voltage gain of the traditional converter through reducing the conduction losses. Furthermore, the five-element resonant converter provides high voltage gain at the resonance frequency and can minimize the circulating energy of the resonant tank. In other case, the five-element LCLCL resonant tank is adopted with half the bride at the primary side. These topologies ease to combine with other output structures such as voltage doubler, full-bridge, and current-doubler structures. The circulating energy of the resonant tank can be reduced largely that lower than the conventional resonant converter [135].

(d) Three port bidirectional multi-element resonant converter, as shown in Figure 16e: This converter transmits more active power to load due to the employment of third order harmonic components and fundamental components. Besides, a non-ideal isolated transformer is considered to be the parasitic leakage inductor is often ignored for the multi-element resonant converter. In this topology, zero voltage switching characteristics for all the three-port power switches can be achieved easily and around 96% power conversion efficiency is achieved. This achieves a more flexible and elegant design compared to the complex decoupling matrices. It is also simple to make digital control implementation for this topology [136].
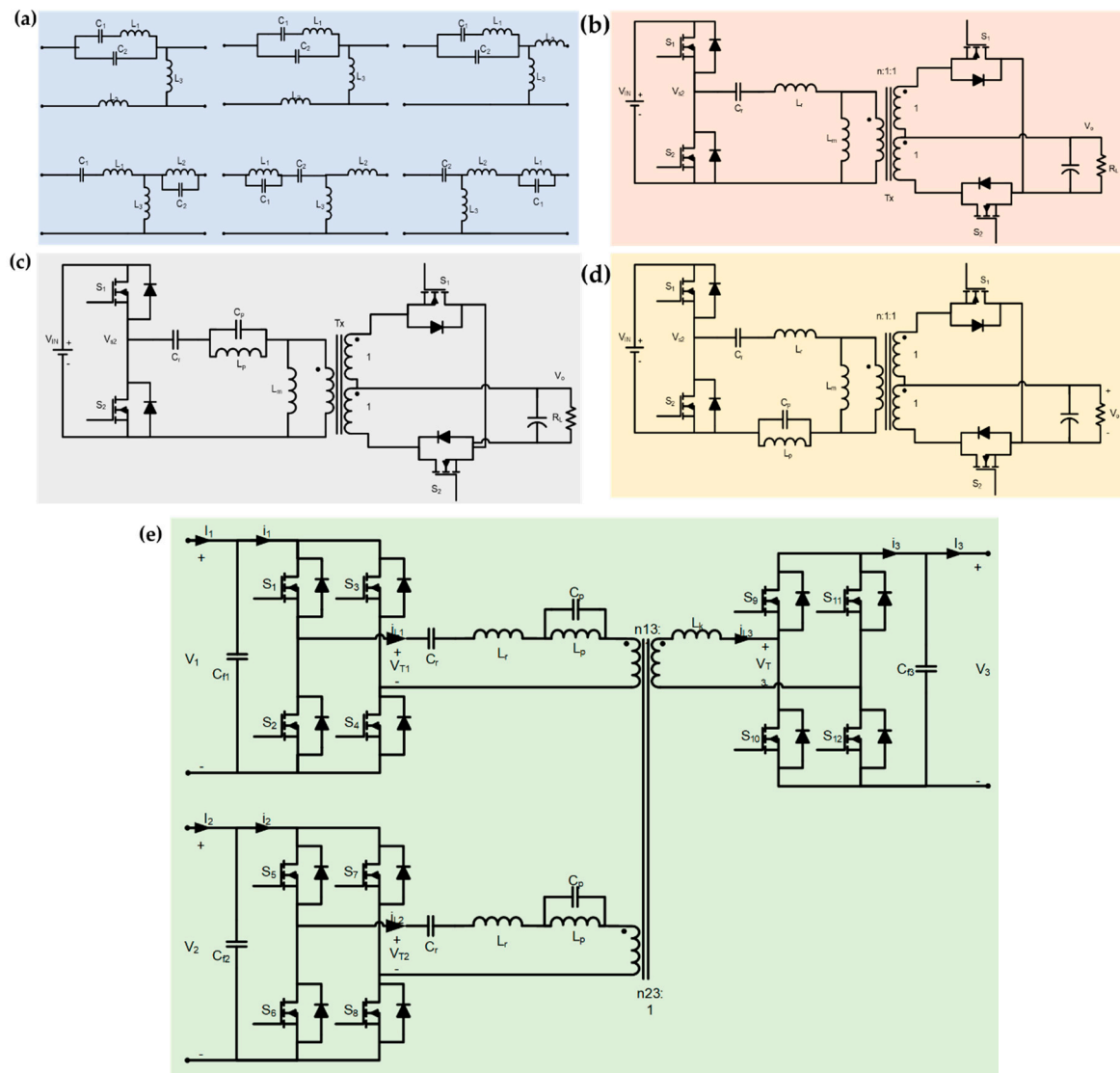
Figure 16. (**a**) Multi-element converter possible connection [130]. (**b**) Three-element LLC resonant converter [132]. (**c**) Four-element LLC resonant converter [134]. (**d**) Five-element LLC-LC resonant converter [135]. (**e**) Bidirectional multi-element resonant converter [136].

4.2.5. Push-Pull Converter Model

Another important model of the DC–DC converter is a push-pull converter, as shown in Figure 17. It is also referred to as a switching converter that changes the DC supplied power with the aid of the transformer. The push-pull converter topology is basically a forward converter operating with the help of primary winding of center tapped. This mainly uses the transformer core effectively when compared with the forward or the flyback converters. Moreover, the copper losses are increased because only half of the copper in the winding is being used at a single time. For available power levels, the push-pull converter possesses smaller filters when compared to the forward converter.

There are some unique characteristics of this converter, such as the main winding of the transformer is fed using the current that is available from the input lines employed by the pair of transistors in a push-pull circuit. These transistors are concurrently switched on and off, sometimes drawing the current in the transformer. Therefore, the current is shattered obtained from the line at the period during the pair of half cycles during the switching condition. Push-pull converters have a stable input current, operated with the low noise at the input and are more efficient for high power applications [137].
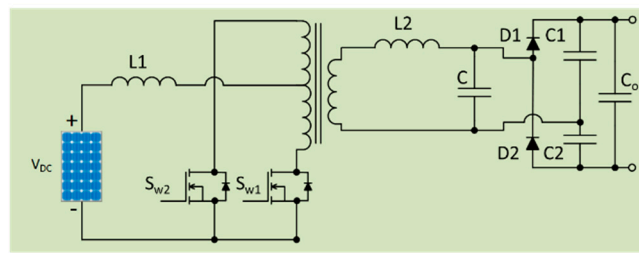
Figure 17. Push-pull converter for PV application [137].

5. MPPT Techniques

Due to the nonlinear current-voltage (I–V) characteristics of the PV panel, tracking the solar power very difficult using the unique type of the maximum power point (MPP) [138]. Atmospheric conditions such as cell temperature and solar radiation and the MPP of the solar panel are not consistent. Therefore, to get the maximum power, the PV panel should be employed at the voltage referring to the MPP and the maximum power point tracker achieve this criterion [139–143]. However, a MPPT is an art of getting the maximum power obtained from the PV panel and it is considered to be a crucial component of the solar PV system. Even though the internal resistance of the PV panel varies with the atmospheric conditions, the load resistance is consistent. Converters controlled with the MPPT algorithm are used to obtain the load matching and achieving the maximum power from the PV panel [144–146].

To ensure that the PV system is working near the MPP, a DC–DC converter with a MPPT controller is employed in between the PV module and the load [147]. There are various MPPT algorithms such as short circuits [148,149]. Open circuit [150–154], control of the ripple correction RCC [155–157], sliding mode control SMC [158–160], perturb and observe (P&O) [161–164], incremental conductance [165–170], fuzzy logic controller FLC [171–177], artificial neural networks (ANN)-based [178–182] were studied and the detail explanation as shown in the following Table 2.

Table 2. Comparison of MPPT techniques for different converters employed in solar PV applications.

Converters	Authors	Control Variable	MPPT Type	Remarks
Buck	Bendib et al. [183]	Duty Cycle	FLC	The author designed a MPPT based on the FLC controller for a buck converter that can control the PV array to employ at the voltage of operation.
	Alabedin et al. [184]	Duty Cycle	ANN	Enhanced performance in the array power after dealing with fluctuations.
	Radhakrishnan et al. [185]	Voltage and current	P&O	The author implemented under low irradiation conditions. Linear current booster (LCB) for a DC motor that can be employed for pumping applications.
	Zhang et al. [186]	Current	Variable inductance	Prior to solar irradiance, the light enhances and inductance decreases. This variable inductance enables to get the continuous current in partial shading and the fewer irradiation conditions.
	Veerachary et al. [187]	Voltage and current	P&O	Designed the coupled inductor scheme to diminish the distortions in the source current. Furthermore, with this design, the core size can be diminished.
Boost	Kwon et al. [188]	Voltage	Hysteresis Loop	Designed a three-level boost converter along with a hysteresis power loop-based MPPT technique. The designed scheme also diminishes the ripples in the source current, the losses in the diodes and the stress on switches.
	Choi et al. [189]	Voltage and Current	P&O	Designed a high gain boost converter equipped with the floating output that decreases the stress on the switches and lowers the ripples in the currents both in the input and the output currents and decreases the voltage and current ratings of the various components.
	Elshaer et al. [190]	Voltage and Current	FLC-GA	Here, the PID controller under various load conditions is accordingly tuned with the GA and the FLC-based controller to automate the tuning process.
	Veerachary et al. [178]	Voltage	FLC with ANN	The designed feedforward FLC MPPT technique uses an ANN that supports it as an optimizer. To define the reference voltage on-line, the BP algorithm is trained by the ANN enhancing the tracking performance.
	Agorreta et al. [191]	Voltage and current	FLC	The designed outer loop controls the input voltage. Pertaining to the fuzzy switching technique, the inner loop topology controls the inductor current that can be enabled to operate in mixed conduction mode.
Buck-boost	Ishaque et al. [192]	Duty Cycle	PSO	Under partial shading conditions, the designed PSO algorithm is applied for the MPPT that showed the tracking efficiency of 99.5%.
	Wu et al. [193]	Voltage and Current	P&O	FLC-based single-stage converter is designed for Solar PV powered applications such as Solar PV powered lighting. The integrated SSC is operated with the bidirectional buck–boost charger/ discharger along with the class D series resonant parallel loaded inverter.
	Veerachary et al. [194]	Voltage	ANN	Here the gradient descent algorithm is employed for training. Furthermore, the usage is applicable to the permanent magnet series motor.
	Syafaruddin et al. [195]	Irradiance and Temperature	ANN-FLC	Using the high quantity of PSC (passive solar component) data, the three-layered ANN is trained for tracking the GMPP. The GMPP voltage is derived from the ANN. Further the ANN along with integrated FLC along with the polar controller to supply regulate pulses for the buck–boost converter.
	Kuo et al. [196]	Voltage and current	P&O	The designed MPPT carries a voltage ranges from the 12 V DC obtained from the PV panel to 230 V AC from the grid lines. Similar to the conventional voltage the designed converter also possesses one switch and operated with two modes.

Table 2. *Cont.*

Converters	Authors	Control Variable	MPPT Type	Remarks
Cuk	Lin et al. [197]	Voltage and current	P&O	The cuk converter used to charge the battery in the daytime and the forward converter drives the LED. During the discharging time, the forward converter operated the LED.
	Chung et al. [198]	Duty cycle	Injecting sinusoidal pulse	The designed converter works in the discontinuous capacitor voltage mode along with the continuous input current. MPP performs its operation by giving the sinusoidal pulses into the duty cycle and in comparison, with the switching stress and the input voltage variations.
	Mahmoud et al. [199]	Voltage	FLC	Without any modifications in the membership functions, the designed MPP works with the desired efficiency and enhanced robustness when applied for the resistive loads.
	Safari and Mekhilef et al. [200]	Voltage and current	INC	The designed model is simple without any proportional-integral (PI) control loop that can be used to track the peak power.
SEPIC	Duran et al. [201]	Voltage and current	P&O	The SEPIC converter operating in the interleaved mode connected in parallel used for measuring the I-V and P-V properties of a PV panel/module.
	Tse et al. [202]	Voltage	RCC	A minimum sinusoidal perturbation is supplied into the switching pulses to compare the average value of the panel voltage with the ac component.
	Hyun-Lo et al. [203]	Voltage	FLC	When the optimum solar irradiance is not obtained, the FLC controller is used to maintain the charging current to operate the battery at the desired value.
	Rathge et al. [204]	Voltage and current	Pulse-current charging	The designed converter operates with high accuracy and the high efficiency MPP technique to track the maximum power and store energy in the battery. Further the overcharging of the battery is avoided using the pulse charging scheme in the rest of the periods.
Zeta	Salenga et al. [205]	Voltage and current	P&O	The designed topology is based on the transfer functions obtained from the dynamic analysis experimented with the Zeta converter for hybrid solar and wind power systems.
	Priya et al. [206]	Voltage and current	P&O	The adaptive perturbation step is implemented with the necessary step size. The perturbation step size is dominantly low at the initial stage of the tracking and at the operating point, MPP step size decreases.
	Antonio et al. [207]	Voltage and current	P&O	The designed algorithm is used to track the maximum power and the constant voltage /constant current method to monitor the charging and the discharging cycles of the battery.
	Zanotti et al. [208]	Voltage	Input impedance	The implemented technique does not require the storage as the previous value of the resistance is not required.
Flyback	Unal YILMAZ et al. [209]	Voltage	Incremental Conductance (IC)	The flyback converter operates with the incremental conductance method under variable irradiance and temperatures.
	Shanmugave et al. [210]	Voltage and current	P&O	The designed MPPT strategy used a settled step prescient control along with the Model Predictive Control under a measured quick irradiance.
	Dong-Kyun Ryu ey al. [211]	Voltage and current	Current Sensor	The author used a current sensor to track the MPPT point and the designed system found to be simple and cost-effective.
	Mohammed et al. [212]	Voltage and current	Model Predictive Control (MPC)	The major contribution of this paper is the advancement of the P&O through a fixed step predictive control at the faster variations of the solar radiation.

Table 2. *Cont.*

Converters	Authors	Control Variable	MPPT Type	Remarks
Forward	Carlos et al. [213]	Voltage	SMC	The author proposed a sliding mode controller (SMC) operating on each converter to regulate the voltage at the input and outputs to avoid the overvoltage criterion at the partial shading conditions.
	Mustafa Engin Basoglu et al. [214]	Voltage	P&O	The author studied the performance of the forward converter that is evaluated by the perturb and observe (P&O) algorithm for modular level and the submodular level MPPT systems designed in the MATLAB/ Simulink.
	Abdelhamid et al. [215]	Duty cycle	P&O	The author proposed a modified variable step size P&O strategy that can be used to overcome several demerits such as accuracy and the convergence speed at the swiftly changing atmospheric conditions.
Resonant	Akif et al. [216]	Voltage	SMC	The converter operates with the 32-pulse density modulation to attain the desired efficiency of the PV panels and the MPPT by removing some of the control signals.
	Meghana et al. [217]	Voltage	Conventional MPPT	Here the DC voltage is used as the perturbation variable for the LLC resonant converter.
	Andrian et al. [218]	Voltage	Incremental conductance	The implemented conventional maximum power point tracking (MPPT) systems use the pulse width modulation (PWM) for DC–DC converters. Furthermore, the author proposed an incremental conductance method used for the LLC resonant converter.
	Qian et al. [219]	Duty cycle	Conventional MPPT	The proposed algorithm used the boundary frequency ranges to determine the switching frequencies of the resonant power converter.
Push-pull	Luigi et al. [220]	Voltage	P&O	The author proposed the adaptive step P&O algorithm to achieve an excellent dynamic response of the PV array. This is achieved by adapting the perturbation step to the actual conditions of the PV array. This type of converter topology is found to be an efficient interface to enhance the low voltage of the PV arrays and also effectively regulates the flow of power when there are variations in the input and output voltage levels.
	Gaikwad et al. [221]	Duty cycle	Conventional MPPT	The author proposed a hardware implementation of a DC–DC push-pull converter based on the TL598 control to track the maximum power point.TL598 operates with the fixed frequency and variable duty cycle controlled IC that can be employed for the charge controller purposes. This can be achieved from the MPPT algorithm by the variation of external voltage at Pin 4 of Dead Time Control (DTCON) in the TL598 IC. This further enhances the tracking speed and also output power stability.
	L.Piegeri et al. [222]	Voltage	P&O	The author proposed an adaptive P&O method to have faster dynamics and improved stability when compared to the traditional P&O algorithm. This is because when the atmospheric conditions, either constant or slowly varies, the P&O method oscillates nearer to the MPP. Hence this adaptive P&O method was employed in this study.

Table 2. *Cont.*

Converters	Authors	Control Variable	MPPT Type	Remarks
H-Bridge	Mahraz Amini et al. [223]	Voltage	Model Predictive Control (MPC)	The author proposed a technique for the grid-connected Cascaded H-Bridge (CHB) inverters where the DC-link voltage is independently controlled at different insolation conditions.
	Bailu et al. [224]	Voltage	Conventional MPPT	Independent control of the DC-link voltage is encouraged in this work. Furthermore, the generalized nonactive power theory is implemented to generate the nonactive current reference.
	Nawrin et al. [225]	Duty cycle	Incremental Conductance	The author illustrated a control strategy to design and operate the maximum power point tracking (MPPT) in the PV system using the incremental conductance algorithm.
	Mingxuan et al. [226]	Voltage	PSO	The author proposed the grouping method of the shuffles frog leaping algorithm (SFLA) is equipped with the basic PSO algorithm to indicate the swift and precise search of the global extremum. Here, an adaptive speed factor is studied to improve the convergence speed. Furthermore, the PWM algorithm enabled the permuted switching of the available PV sources is implemented.

6. Modulation Strategies

There is a variety of techniques that were analyzed to control the DC–DC converters. Moreover, different control and modulation techniques are used for proper control of the converter to obtain the desired phase, frequency, and amplitude of the voltage and current at the optimum point of the use. The most used techniques for switching control of a switch-mode converter are such as Pulse-width modulation (PWM) and Phase-shift modulation (PSM). Sometimes, the phase-shift modulation is also referred to as phase-shift PWM (PS-PWM). Among these two techniques, the PWM is the most widely used for controlling the switch-mode DC/DC converters in different applications. Furthermore, the PWM is grouped as fixed frequency (FF) and variable frequency (VF) PWM [227]. There are many modulation techniques implemented for the various PV applications of the DC–DC converters as depicted in Table 3.

Table 3. Comparison of different modulation techniques for the DC–DC converters.

Converter	Author	Modulation Technique	Remarks
Buck	Chen et al. [228]	Improved Delta Modulation Technique	The proposed technique for the buck converter, possess various slopes of the carrier signal obtained by the feedforward and from where the control signal is sent to the input control unit to the integrator of the delta modulator.
Buck and Boost	Mandi et al. [229]	Unified Digital Modulation	The author proposed a novel integrated technique i.e., unified digital PWM/PFM scheme to achieve efficiency over a wide operating range and to obtain the controlled transitions. Buck and Boost converters were tested with this technique.
Buck	Boudoudas et al. [230]	Dual Randomized Pulse Width Modulation	This technique aims to reduce the potential harmonics, the effect of electromagnetic interference (EMI) and the uniform distribution of the power spectrum. The DRPWM scheme integrated by the photovoltaic source and its operation in the discontinuous conduction mode is studied. From this technique, the steady-state characteristics were obtained for the buck converter.
Buck	Nguyen et al. [231]	Chaotic Pulse Width Modulation	The author proposed a voltage controlled buck converter to diminish the electromagnetic interference (EMI) using the pulse width modulation (PWM) technique that relies on the chaotic triangular ramp generator. Without the implementation of the EMI filters, the proposed converter reduces the effect of the EMI when operated in the chaotic mode.
Boost	Diab et al. [232]	Modified modulation scheme	In this paper, the author discussed a modified modulation scheme employed for the three-phase boost converter that is used for the controlling of both active and reactive powers that are injected into the grid. Furthermore, it is used to reduce the voltage stress on the capacitors and the switching devices.
Boost	Parveen et al. [233]	Sinusoidal pulse width modulation	Here the author proposed the system for the interleaved boost converter, characteristics that can be controlled by using the maximum power point tracking (MPPT) algorithm and further the voltage control of the inverter can be modulated using the sinusoidal pulse width modulation technique. The proposed system removes power losses.
Buck-boost	Marrison et al. [234]	Novel modulation technique	The author discussed the novel modulation technique used for a power factor correction (PFC) used for an isolated AC/DC converter that is obtained by the integration of the non-isolated converter such as two switch buck–boost AC/DC converter with the implementation of the dual active bridge DC/DC converter (2SBBDAB).
Cascaded, bidirectional, buck–boost converters	Stefan et al. [235]	Zero voltage switching (ZVS) modulation technique	Here the author, mentioned a novel reduced loss, with constant frequency, zero voltage switching (ZVS) modulation technique for the cascaded, bidirectional, buck–boost converters that are employed in the hybrid electric vehicles and in fuel cell vehicles (FCVs).
SEPIC	Nan li et al. [236]	PWM-Based Sliding Mode Controller	The author used the principle of the PWM-Based Sliding Mode Controller that can be used for a SEPIC converter and for the effectiveness of the control algorithm developed for embedded applications such as FPGA, ASIC, etc. Here various constraints such as the Silicon surface and the reduction factor are the key factors.
SEPIC	Mohanraj et al. [237]	Sinusoidal pulse width modulation technique	Here, the author designed a SEPIC converter with the PV panel that is controlled by the sinusoidal pulse width modulation technique along with the PI controller for the control of the duty cycle ratio of the converter.
SEPIC	Emre et al. [238]	–	Here the author, represented the control technique for the modified SEPIC converter to achieve the high voltage ratio by the passive components.
Zeta and the SEPIC	Adriano et al. [239]	Pulse width modulation	The PWM is used for the isolated bidirectional DC–DC converter, depending on the dual properties in between the Zeta and the SEPIC converters.
SEPIC	Bawane et al. [240]	Pulse width modulation	Here the author discussed the topology of the power conversion circuit of a DC–DC SEPIC converter implemented by the pulse width modulation strategies.
SEPIC	Hu et al. [241]	Hysteretic override technique	The author used a hysteretic override technique that enabled the converter to deny the load distortions along with the bandwidth that is much greater than the modulation frequency in order to limit the output voltage disturbances to a fixed value.
Buck-boost	Feng et al. [242]	Phase opposing and disposition type of modulation	The author developed a front end circuitry of Cuk derived from the buck–boost two-level inverter, using the alternative phase opposing and disposition type of modulation scheme. Moreover, the buck–boost three-level inverters can also work to switch as five-level line voltage and three-level phase voltage employing the switches that are active destinated circuits of voltage boost section.
Cuk	Raghavendra et al. [243]	Pulse area modulation strategy	The author employed the variable pulse area modulation strategy to control the voltage at the end of the Cuk converter.
Cuk	Krishnakumar et al. [244]	Randomized pulse width modulation	The author used the randomized pulse width modulation (RPWM) strategy as an efficient technique to diminish the electromagnetic interference on the Cuk converter.

Table 3. *Cont.*

Converter	Author	Modulation Technique	Remarks
Cuk	Fuad et al. [245]	Pulse width modulation	In this paper, the author developed a stabilizing controller with the state space average model of a DC–DC converter that was pulse width modulated does not resemble a stabilizing controller for the DC–DC converter itself, particularly in the Cuk converter case.
Cuk	Mehrnami et al. [246]	Discontinuous modulation scheme	Here the author discussed the discontinuous modulation scheme (DMS) for the usage of DTCI in which deactivates the one module at the resulting time in the inverter's modules discontinuous operation.
Flyback	Marlon et al. [247]	Alternative modulation strategy	The author employed the alternative modulation strategy for the usage of the flyback converter along with the differential output connection.
Flyback	Dan et al. [248]	Leading-edge modulation	The author implemented a leading-edge modulation, i.e., at the clock signal pulse width modulation (PWM) signal turns off and it is turned on when the error signal crosses the ramp waveform. It is also shown that the positive zero during the power stage of the transfer function of both the boost and the flyback regulators can be moved under suitable conditions to the left side of the plane.
Flyback	Yang et al. [249]	Pulse width modulation	The author implemented a novel dual-type DC–DC fly back converter operated with leakage energy recycling. In this type of converter, the only active switch is used and the PWM technique is used to control this switch along with the two transformers.
Dual active bridge (DAB) converter	Byeng et al. [250]	Pulse width modulation	Here the author discussed the single pulse-width modulation topology using a soft-switching technique operated for a broad range of the output voltages obtained from the bidirectional dual active bridge (DAB) converter.
Dual active bridge (DAB) converter	Muhammed et al. [251]	Combined pulse-width modulation (CPWM)	The author proposed two important modulation techniques such as the single pulse width modulation and the dual pulse width modulation that were combined into the one modulation strategy usually referred to as the combined pulse-width modulation (CPWM).
Cascaded H-bridge converter	Xiao et al. [252]	Pulse width modulation	The author analyzed the relationship between the PS-PWM and PDPWM for the cascaded H bridge converter along with the enhanced hybrid modulation topology.
–	Sudha et al. [253]	Carrier-based pulse width modulation technique	Here the author discussed a method using the fundamental switching and the carrier based on pulse width modulation techniques. The main feature of this method is to reduce the total harmonic distortions (THD), certain switching and the heat losses. The developed technique is formulated in order to enable the fundamental switching along with the carrier-based pulse width modulation technique.
H-bridge	Lewicki et al. [254]	Space vector modulation	The author selected an appropriate H-bridges and the control of these bridge duty cycles using the space vector modulation (SVM) algorithms for balancing the voltages of the DC-link. This technique enabled to maintain the constant voltage in all the capacitors in the inverter. To the balancing function, even though the DC-link voltages are not properly balanced, the output voltage vector is normally generated from the SVM strategy.
LLC type Resonant	Deck et al. [255]	Hybrid modulation strategy	Here the author proposed a new type of modulation strategy for the LLC type Resonant converters that were implemented in the solar applications. The technique depends upon the zero current crossings in the resonant tank. By controlling a single parameter, the input to the output voltage ratio can be controlled by not losing the property of soft switching.
LLC type Resonant	Dick et al. [256]	Optimized buck mode modulation strategy	In this paper, the author presented an improved modulation strategy. This technique depends upon the resonant current zero-crossing. This model depends upon the simulation of the converter that automatically varies with the parameters of the converter.
Push-pull converter	Soubache et al. [257]	Pulse width modulation	The voltage regulation in this paper is achieved by the pulse width modulation (PWM) technique by adding a secondary side bidirectional AC switch to the resonant converter for the wide range of the input voltage that is more beneficial for the photovoltaic applications.
Forward flyback	Yu et al. [258]	Dual constant on-time modulation	This modulation technique is used in order to obtain high efficiency across the wide load and the input range. Zero current switching is obtained when the main switch is in ON state for half a period of the constant resonance for the forward diode. Furthermore, to reduce the dead time among the output diodes. Moreover, zero voltage switching can be obtained when the auxiliary switch is turned ON for very little interval of time. The proposed design is more applicable for the PV systems of tree type.

7. Comparative Performance Assessment

The studies on performance of the converters is very essential while choosing the converter for their application in PV systems. Taghvae et al. [259] discussed the buck, boost, buck–boost, Cuk and SEPIC DC–DC converters implemented for the photovoltaic systems along with the maximum power point tracking algorithms. Furthermore, the performance of the individual DC–DC converters was shown to achieve the maximum power point operation. Eventually, the author concluded that the buck–boost converter is applicable for its operation in any available solar irradiation and the load condition to yield the maximum power point operation. Farhat et al. [260] described the effect of the variation of the solar irradiance and the cell temperature on the selection and the design of the various converter topologies that are widely used in the PV systems. From this analysis, it is lucid that the buck–boost and the cuk converters can deliver the optimal performance. The filter capacitance should be greater than that of the boundary capacitance maximum value to diminish the ripple in the output voltage.

In comparison with the other non-isolated converters, the buck–boost converter shown the reasonable input and the output power rating above which that the converter's efficiency reduces as an increase in the power ratings. Whereas the Ultra-lift Luo converter has a higher efficiency when the input and the output power ratings are found to be higher. Concurrently, the super-lift, cuk and the SEPIC converters are majorly applied to the medium power applications and it is observed that the buck–boost converter is best suited for the applications of low power utilities.

When high power renewable energies are considered, it is always better to use the ultra-lift Luo converter as it delivers the higher efficiencies for industrial applications and it proved experimentally in [87,260], but ultra-lift Luo converter is similar to the buck–boost and cuk converters as they produce the inverted output with respect to the input voltage. The ultra-lift Luo DC–DC converter (elementary circuit) is enhanced when compared to the other converters, the voltage stress on the switch is large enough so that the duty ratio also increases; whereas this directly increases the cost as well as the ratings of the power semiconductor switch [261].

Furthermore, there are many isolated converters that yield appreciable performance when employed with solar PV systems. The following Table 4 illustrates the performance of various isolated DC–DC converter that can be used in the solar PV system applications.

Table 4. Comparative performance of the isolated DC–DC converters employed in solar PV applications.

Author	Converter	Frequency	Power	Efficiency	Remarks
Lessing et al. [247]	Bidirectional flyback converter with Differential output	20 kHz	500 W	86.4% (Alternative Switching) 83.4% (Complementary Switching)	As might be expected, the proposed alternative switching method has higher efficiency gain than the complementary switching method applied to the same prototype. The results of the open-loop show that this converter, which operates on both techniques, presents a solution for a simple application that does not require a closed-loop control in the case of an off connection.
Sable et al. [248]	Flyback converter with leakage energy recycling	75 kHz	250 W	94.8%	This converter is a simple structure and low cost. the converter uses two transformers with the equal inductance. During the switch-off, the magnetized inductance of the transformer is released to the output. At the same time, the energy dispersion of the transformers can be recycled.
Yang et al. [249]	Bidirectional Dual Active Bridge Converter	10 kHz	50 kW	85.6% ~ 97.5%	It represents integrated algorithm techniques for controlling the PWM signal. The purpose of this method was to provide soft switching in the whole operating range by PWM patterns.
Byen et al. [250]	Dual Active Bridge Converter	40 kHz	100 W	82% ~ 92%	The modified a DPWM to overcome hard switching operations with the previously proposed (CPWM) modulation approach. the DPWM is evaluated to operate throughout the ZVS including the current leakage inductance. The DPWM modification includes the consideration of adding parameters to satisfy current leakage inductance conditions.
Malek et al. [251]	Cascaded H–Bridge Inverters	610 Hz	–	Slightly reduce in the efficiency	A modulation strategy was proposed combining PS-PWM and PD-PWM to improve the output quality of the output line voltage for CHB inverters. An uncontrolled modulation approach that can reduce frequency transfer to theoretical value is offered for multilevel inverters.
Xiao et al. [252]	Seven levels Cascaded H–Bridge Inverters	7 KHz	570 KW	Maximum efficiency is produced	The proposed SVM method allows maintaining the same voltage level across all inverter capacitors. Regardless of the balancing function, the SVM strategy allows the output voltage vector to form correctly even if the intermediate circuit voltage is not balanced.
Deck et al. [255]	LLC type resonant converter	Variable frequency	–	–	This paper focused on the control system of the converter by varying and comparing the frequency and phase-shift modulation
Yu et al. [258]	Inductor less forward flyback converter	1 MHz	250 W	97%	The PWM flyback converter and a hybrid resonant inductor less with forward and double-time constant modulation, in which the inductor less forward converter works at full resonance with minimum idle time, while the flyback converter works in a piecewise linear.

## 8. Advances in DC–DC Converters for PV Systems

There are various recent advances in the field of the converters applied for the PV systems. As discussed earlier the DC–DC conversion schemes are generally employed to fix the voltage range of the photovoltaic array to the PV inverter and at the same time develop the MPPT control.

The recent growth of interest pertaining to the PV topologies is the Module Integrated Converters (MIC). These MICs can be generally understood as the step-up DC–DC converter exhibiting the higher efficiencies. The MICs are self-powered and isolated galvanically for the autonomous control and to track the maximum power point of the PV panel output. In [262], the integrated synchronous boost converter and the series resonant DC–DC converter (SRC) was studied (Figure 18). The main advantage of this type of construction is to offer high efficiency because of no switching losses that are obtained by the zero voltage switching (ZVS), further, the high power density is obtained by the bidirectional core excitation.
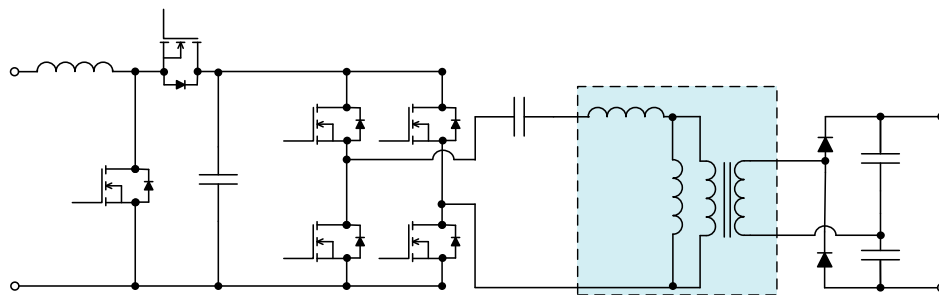
Figure 18. Asynchronous boost and a series -resonant converter exhibiting the two-stage topology [263].

Furthermore, the above structure can be simplified by replacing the passive impedance network in place of boost converter as shown in Figure 19 [263]. This network consists of various components such as capacitors, diodes, and inductors to obtain a special configuration. The variation of the PV panels output voltage is regulated by adapting the shoot-through duty cycle. Later the voltage of constant amplitude is supplied to an isolation transformer. The DC–DC converter of impedance source [264] that takes extension using the series resonant network can diminish the switching frequency range and will result in the enhanced efficiencies. Furthermore, because of the inherent short circuit defense, reliability can be increased drastically.
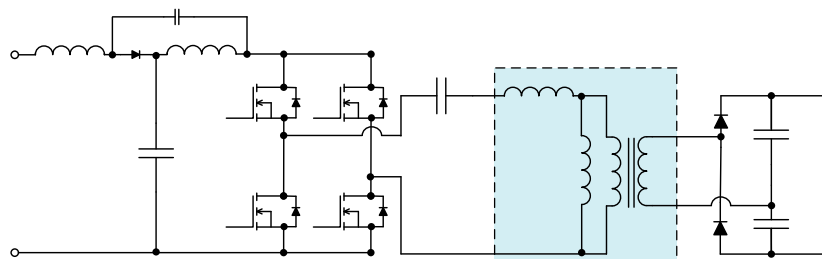
Figure 19. Quazi-Z source resonant converter [264].

There are many varied approaches that were studied recently to overcome the problem of efficiency optimization when operated over the wide input voltage range. For instance, in [265] the more efficient multi-resonant DC–DC converter was designed that was illustrated in Figure 20. Though its structure is complex, during the design of the resonant tank, the converter has the minimum number of the external discrete components. Furthermore, the series inductance can be realized using the leakage inductance and parallel inductances can be realized by the magnetizing inductance of the isolation transformer. The sum of all the parasitic capacitances constitutes to form the parallel capacitance C_p of the isolation transformer and the rectifying diodes. Here the carefully employed resonant tank leads to greater efficiencies operated over a wide range of the input voltage.
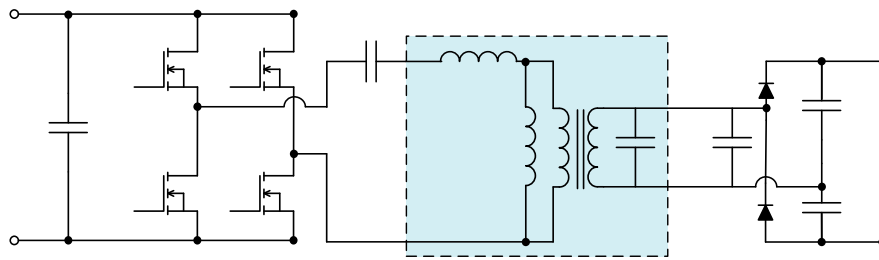
Figure 20. LLCC series-parallel resonant converter [265].

A novel resonant converter topology is illustrated in Figure 21, which operates depending on the panel operation conditions in dual resonant modes. This enables maintaining high efficiency over wide inputs of voltages at various levels of the output power [266]. The novelty of this circuit is that a half-wave rectifier is located at the secondary side of the transformer. Enabling the half-wave rectifier along with the voltage doubler rectifier of the main circuit, the output voltage is found to be enhanced. The converter efficiency is almost 97% when the converter features of both the ZVS for the primary side switches and at the same time zero current switching (ZCS) for the rectifier diodes in both the resonance modes.
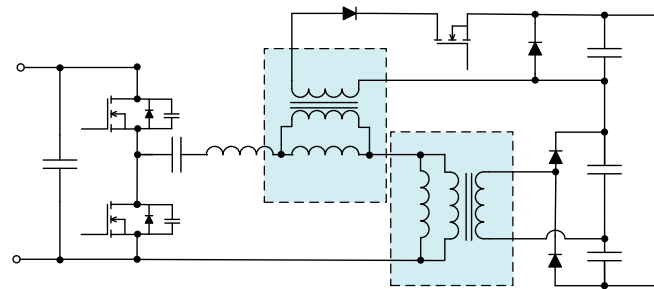

Figure 21. Dual-mode resonant converter [266].

One more approach for the highly efficient resonant converter is obtained by adding the bidirectional AC switch upon the secondary winding of the isolation transformer as shown in Figure 22. To provide the wide input voltage regulation at the greater range of the input voltage and the output power [267], the higher energy efficient series converter is incorporated with the pulse-shift modulated full-bridge buck converter and the pulse width modulated boost converter. Furthermore, the converter features the zero voltage and/or zero current switching at the switching primary side and the zero current switching's at the rectifier diodes that result in the enhanced efficiencies.
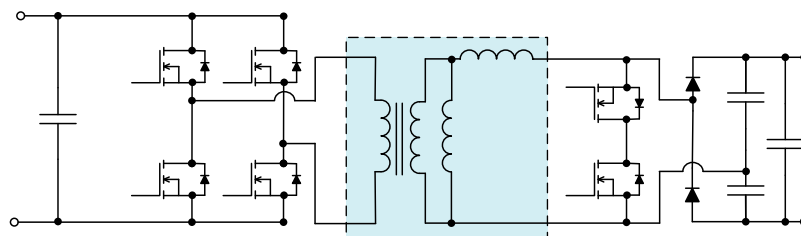

Figure 22. Series resonant converter with the bidirectional AC loads [267].

The highly efficient half-bridge LLC DC–DC converter as shown in Figure 23, possesses a more appreciable advantage because of the use of a minimum number of switches on the primary side that results in the simple structure. As discussed in the previous cases, the LLC resonant tank is formed by the leakage and magnetizing inductances of the isolation transformers along with the outer resonant capacitor. Therefore, the zero voltage switching is achieved by the power switches and the zero current switching's are achieved by the external diodes at the output over a wide range of the load [268].

Generally, with the aid of the voltage doubler rectification, the feasible turns ratio of the isolation transformer results in the high voltage gain.
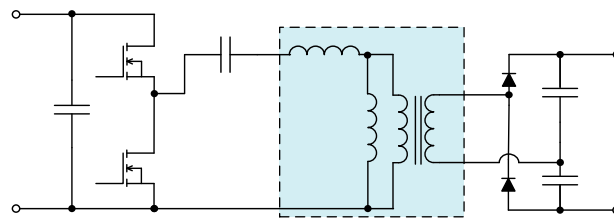

Figure 23. Half-bridge LLC resonant converter [268].

Another novel model of the module integrated converter is the soft switching current-fed push-pull converter that is shown in Figure 24 [269]. The main advantage of this type of converter is the current minimum stress on the input current, enhanced voltage gain and low conduction and switching losses. The unique feature of this converter is the existence of the parallel resonance between the leakage inductance at the secondary side of the isolation transformer and the resonant capacitor. Here the transistors are switched on and off at the conditions of the zero voltage and the zero currents. Moreover, at the zero current condition, the rectifier (voltage doubler) diodes are also turned off.
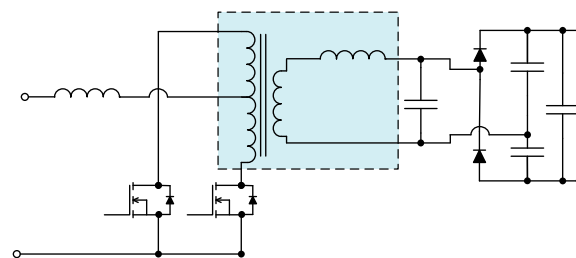
Figure 24. Parallel resonant current-fed push-pull converter [269].

The low-cost interesting topology of the module integrated converters was studied in [270]. The traditional two inductors isolated boost converter was developed using the snubber of the non-dissipative regenerative type including the control of the hysteresis and the constant duty cycle Figure 25. The magnetizing, leakage and the resonant capacitor constitute to form the multi resonant tank was introduced. The appreciable features obtained from these modifications are the minimum input current ripple, zero current switching conditions both for the switches at the input and the diodes at the rectifier and the enhanced light load property.
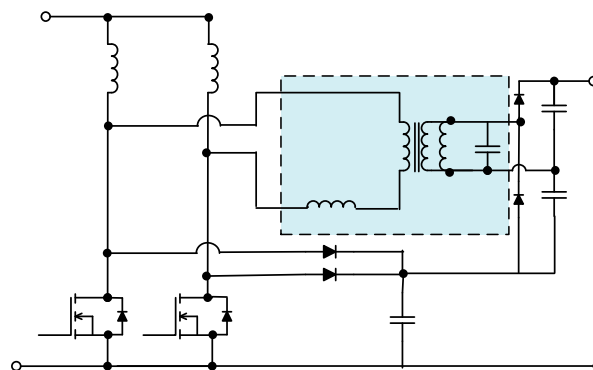
Figure 25. Multi resonant two inductor boost converter with non-dissipative regenerative snubber [270].

Table 5 illustrates the unique specifications of some emerging experimental DC–DC converter topologies for PV system applications for which the detailed description can be obtained from [262,264–270].

Table 5. Key specifications of the recently advanced DC–DC converter topologies for PV systems.

Figure	Maximum Power (W)	PV Panel Voltage (V)	DC Bus Voltage (V)	Voltage Gain Range (Input) (V)	Switching Frequency (kHz)	Efficiency (%)	Number of Switches	Number of Diodes	Resonance Type
18	275	15–45	400	8.9–26.7	210 (boost) 350 (SRC)	97	6	2	Series
19	500	50–150	100	0.7–2	49.3	96	4	3	Series
20	244	20–35	700	20–35	215–268.5	96	4	2	LLCC
21	300	15–35	320	5.6–21.3	130	97.4	6	2	Series
22	240	22–40	400	10–18.2	76–185	96.5	3	4	LLC
23	200	24–48	380	7.9–15.8	100	95.4	2	2	LLC
24	250	20–40	400	10–20	50–100	96.6	2	2	Parallel
25	210	26.6	350	13.2	100	93.6	2	4	LLC

9. Conclusions

In the light of many mentioned problems pertaining to the converter topologies and their selection for the PV system applications, the isolated and non-isolated converters discussed in this review are the most important components for the efficient interface and delivery of the solar PV energy to the utility. A detailed study was done on the analysis of different topologies for their operation in the PV applications. The following mentioned problems can be summarized based on the research that can be obtained from the literature.

There is a great interest in maximizing the solar energy generation to meet the drastic rise in demand. The most popular way to achieve this is by employing both the DC–DC converters and the MPPTs. It is observed that the buck converter and the boost converter are found to be the effective topologies at the available price. The main drawback of these converters is that they possess the problem in the tracking under various combinations of the load, radiation, and the temperature.

The other non-isolated converter topologies such as the buck–boost, SEPIC and cuk converters can achieve optimal efficiencies and are ideal to operate for the MPPT applications since they do not rely on the radiation and the temperature that enables them to achieve the maximum point. The main disadvantage of the cuk and the SEPIC converters is that they possess higher reactive components. Though they operate with greater efficiencies, the main drawback also relies on their higher cost. Among many non-isolated converters, it is observed that the buck–boost converter is the best application of the low power loads because of its higher performance and the lower power losses. Thus, a buck–boost converter is the best suited one for the low power applications such as the solar PV systems, PM (permanent magnetic) DC motors, low power solar-based stepper motors, etc. Similarly, the positive-output super-lift Luo and the ultra-lift Luo converters possess higher efficiencies and the lower switching losses that can be used when there is a large voltage step-up is required from the low voltage sources. The optimal performance of these two converters can be obtained when operated at the constant duty ratio. Since the efficiency, loss, and stress on the switching elements are moderate in the SEPIC and the cuk converters so that they are used for the medium power utilities.

Furthermore, it is identified that the cascaded structures of the converter topologies can enhance the gain of the voltage and enable to obtain the lower ripple contents. The main disadvantage of this type of converter structure is the higher noise of EMI and lesser efficiencies. Moreover, the inductor coupled in the converter topologies uses the energy storage obtained from the magnetizing core inductances levels up the voltage gain. This also diminishes the current stress on the switching components. Furthermore, the operation of the converters in the DCM (discontinuous mode) minimizes the commutation losses and enable them to obtain less ripple-free input current.

This paper also reviewed the different MPPT techniques of various converters as mentioned in the tabular comparison. It is observed that the selection of the MPPT tracking method is unique and independent of the type of converter topology. P&O is the best preferred MPPT technique. From the tabular comparison, it is found that the buck–boost, SEPIC, cuk, and zeta converters can track MPP more efficiently. The elaborated description of MPPT techniques and modulation strategies of various isolated converters such as fly back, forward, resonant, push-pull and bridge type of converter were analyzed extensively. The performance comparison of both the isolated and non-isolated converters implemented in the solar PV systems was studied.

Furthermore, there are some recent advances in the power electronic converters that can be employed for solar PV applications, were explained with the detailed description, and their elemental analysis was represented with great precision. In the coming near future, it is forecasted that the performance of the solar PV system is supposed to enhance, and the cost can be minimized. Depending on the specified power necessity, this review article will assist and can be considered to be a convenient reference for the researchers and engineers in choosing the most adequate and suitable converter topology used for the solar PV applications.

References

1. Khare, V.; Nema, S.; Baredar, P. Status of solar wind renewable energy in India. *Renew. Sustain. Energy Rev.* **2013**, *27*, 1–10. [CrossRef]

2. Nagayoshi, H. I-V curve simulation by multi-module simulator using I-V magnifier circuit. *Sol. Energy Mater. Sol. Cells* **2004**, *82*, 159–167. [CrossRef]

3. Zeb, K.; Islam, S.U.; Din, W.U.; Khan, I.; Ishfaq, M.; Busarello, T.D.C.; Ahmad, I.; Kim, H.J. Design of Fuzzy-PI and Fuzzy-Sliding Mode Controllers for Single-Phase Two-Stages Grid-Connected Transformerless Photovoltaic Inverter. *Electronics* **2019**, *8*, 520. [CrossRef]

4. Gaikwad, K.; Lokhande, S. Novel maximum power point tracking algorithm (MPPT) for solar tree application. In Proceedings of the 2015 International Conference on Energy Systems and Applications, Pune, India, 30 October–1 November 2015; pp. 189–193.

5. Available online: https://www.iea-shc.org/Data/Sites/1/publications/task16-photovoltaics_in_buildings-full.pdf (accessed on 13 December 2019).

6. Dong, L.; Fujing, D.; Yanbo, W.; Zhe, C. Improved Control Strategy for T-type Isolated DC/DC Converters. *J. Power Electron.* **2017**, *17*, 874–883.

7. Wai, R.J.; Lin, C.Y.; Duan, R.Y.; Chang, Y.R. High-efficiency dc-dc converter with high voltage gain and reduced switch stress. *IEEE Trans. Ind. Electron.* **2007**, *54*, 354–364. [CrossRef]

8. Gu, B.; Dominic, J.; Lai, J.S.; Zhao, Z.; Liu, C. High boost ratio hybrid transformer DC-DC converter for photovoltaic module applications. *IEEE Trans. Power Electron.* **2013**, *28*, 2048–2058. [CrossRef]

9. Olalla, C.; Clement, D.; Rodriguez, M.; Maksimovic, D. Architectures and control of submodule integrated dc-dc converters for photovoltaic applications. *IEEE Trans. Power Electron.* **2013**, *28*, 2980–2997. [CrossRef]

10. Huusari, J.; Suntio, T. Origin of cross-coupling effects in distributed DC-DC converters in photovoltaic applications. *IEEE Trans. Power Electron.* **2013**, *28*, 4625–4635. [CrossRef]

11. Bhattacharjee, S.; Saharia, B.J. A comparative study on converter topologies for maximum power point tracking application in photovoltaic generation. *J. Renew. Sustain. Energy* **2014**, *6*, 053140. [CrossRef]

12. Ahmed, N.A. Advanced energy conversion system using sinusoidal voltage tracking buck–boost converter cascaded polarity changing inverter. In *Proceedings of the AIP Conference Proceedings*; American Institute of Physics: College Park, MD, USA, 2011; Volume 48, p. 1337.

13. Ribeiro, E.; Cardoso, A.J.M.; Boccaletti, C. Fault-tolerant strategy for a photovoltaic DC–DC converter. *IEEE Trans. Power Electron.* **2013**, *28*, 3008–3018. [CrossRef]

14. Myers, I.T.; Baumann, E.D. Multimegawatt inverter/converter technology for space power applications. In *Proceedings of the AIP Conference Proceedings*; American Institute of Physics: College Park, MD, USA, 1992; Volume 246, p. 401.

15. Caro, J.C.R.; Maldonado, J.C.M.; Bautista, R.F.V.; Gonzalez, A.V.; Cabrera, R.S.; Resendiz, J.E.V. Hybrid Voltage-Multipliers Based Switching Power Converters. In *Proceedings of the AIP Conference Proceedings*; American Institute of Physics: College Park, MD, USA, 2011; Volume 29, p. 1373.

16. Peng, F.Z.; Li, H.; Su, G.J.; Lawler, J.S. A new ZVS bidirectional DC-DC converter for fuel cell and battery application. *IEEE Trans. Power Electron.* **2004**, *19*, 54–55. [CrossRef]

17. Chen, Y.; Huang, A.Q.; Yu, X. A High Step-Up Three-Port DC–DC Converter for Stand-Alone PV/Battery Power Systems. *IEEE Trans. Power Electron.* **2013**, *28*, 5049–5062. [CrossRef]

18. Zhu, Y.; Xiao, W. A comprehensive review of topologies for photovoltaic I-V curve tracer. *Sol. Energy* **2020**, *196*, 346–357. [CrossRef]

19. Rehman, Z.; Al-Bahadly, I.; Mukhopadhyay, S. Multiinput DC–DC converters in renewable energy applications—An overview. *Renew. Sustain. Energy Rev.* **2015**, *41*, 521–539. [CrossRef]

20. Sivakumar, S.; Sathik, M.J.; Manoj, P.S.; Sundararajan, G. An assessment on performance of DC–DC converters for renewable energy applications. *Renew. Sustain. Energy Rev.* **2016**, *58*, 1475–1485. [CrossRef]
21. Khosrogorji, S.; Ahmadian, M.; Torkaman, H.; Soori, S. Multi-input DC/DC converters in connection with distributed generation units—A review. *Renew. Sustain. Energy Rev.* **2016**, *66*, 360–379. [CrossRef]
22. Zhang, N.; Sutanto, D.; Muttaqi, K.M. A review of topologies of three-port DC-DC converters for the integration of renewable energy and energy storage system. *Renew. Sustain. Energy Rev.* **2016**, *56*, 388–401. [CrossRef]
23. Sri Revathi, B.; Prabhakar, M. Non isolated high gain DC–DC converter topologies for PV applications—A comprehensive review. *Renew. Sustain. Energy Rev.* **2016**, *66*, 920–933. [CrossRef]
24. Arunkumari, T.; Indragandhi, V. An overview of high voltage conversion ratio DC–DC converter configurations used in DC micro-grid architectures. *Renew. Sustain. Energy Rev.* **2017**, *77*, 670–688. [CrossRef]
25. Dileep, G.; Singh, S.N. Selection of non-isolated DC–DC converters for solar photovoltaic system. *Renew. Sustain. Energy Rev.* **2017**, *76*, 1230–1247.
26. Reshma Gopi, R.; Sreejith, S. Converter topologies in photovoltaic applications—A review. *Renew. Sustain. Energy Rev.* **2018**, *94*, 1–14. [CrossRef]
27. Hossain, M.Z.; Rahim, N.A.; Selvaraj, J. Recent progress and development on power DC–DC converter topology, control, design and applications: A review. *Renew. Sustain. Energy Rev.* **2018**, *81*, 205–230. [CrossRef]
28. Amir, A.; Amir, A.; Che, H.S.; Elkhateb, A.; Rahim, N.A. Comparative analysis of high voltage gain DC–DC converter topologies for photovoltaic systems. *Renew. Energy* **2019**, *126*, 1147–1163. [CrossRef]
29. Al-Maamary, H.M.S.; Kazem, H.A.; Chaichan, M.T. Changing the energy profile of the GCC states: A review. *Int. J. Appl. Eng. Res.* **2016**, *11*, 1980–1988.
30. Denholm, P.; Margolis, R.M. Evaluating the limits of solar photovoltaics (PV) in traditional electric power systems. *Energy Policy* **2007**, *35*, 2852–2861. [CrossRef]
31. Zeb, K.; Uddin, W.; Khan, M.A.; Ali, Z.; Ali, M.U.; Christofides, N.; Kim, H.J. A Comprehensive Review of Inverter Topologies and Control Strategies for Grid Connected Photovoltaic System. *Renew. Sustain. Energy Rev.* **2018**, *94*, 1120–1141. [CrossRef]
32. Wind Energy and Solar|Installed GW Capacity-Global and by Country. Available online: http://www.fi-powerweb.com/Renewable-Energy.html (accessed on 2 October 2019).
33. Zeb, K.; Khan, I.; Uddin, W.; Khan, M.A.; Sathishkumar, P.; Busarello, T.D.C.; Ahmad, I.; Kim, H.J. A Review of Recent Advances and Future Trends of Transformerless Inverter Structures for Single-Phase Grid-Connected Photovoltaic Systems. *Energies* **2018**, *11*, 1968. [CrossRef]
34. Yusivar, F.; Farabi, M.Y.; Suryadiningrat, R.; Ananduta, W.W.; Syaifudin, Y. Buck-converter photovoltaic simulator. *Int. J. Power Electron. Drive Syst.* **2011**, *2*, 156–167. [CrossRef]
35. Rashid, M.H. *Power Electronics Handbook*; Academic Press: New York, NY, USA, 2001.
36. Mohan, N.T.; Undeland, M.; Robbins, W.P. *Power Electronics: Converters, Applications and Design*, 3rd ed.; John Wiley & Sons: New York, NY, USA, 2004.
37. Elgendy, M.A.; Zahawi, B.; Atkinson, D.J. Assessment of perturb and observe MPPT algorithm implementation techniques for PV pumping applications. *IEEE Trans. Sustain. Energy* **2012**, *3*, 21–33. [CrossRef]
38. Masoum, M.A.S.; Badejani, S.M.M.; Fuchs, E.F. Microprocessor-controlled new class of optimal battery chargers for photovoltaic applications. *IEEE Trans. Energy Convers.* **2004**, *19*, 599–606. [CrossRef]
39. Saravana Ilango, G.; Srinivasa Rao, P.; Karthikeyan, A.; Nagamani, C. Single-stage sine-wave inverter for an autonomous operation of solar photovoltaic energy conversion system. *Renew. Energy* **2010**, *35*, 275–282. [CrossRef]
40. Femia, N.; Granozio, D.; Petrone, G.; Spagnuolo, G.; Vitelli, M. Optimized one-cycle control in photovoltaic grid connected applications. *IEEE Trans. Aerosp. Electron. Syst.* **2006**, *42*, 954–972. [CrossRef]
41. Peyman, K.; Syyed, M.M.; Morteza, D.; Motab, A.; Amirhossein, M. A High Efficiency DC/DC Boost Converter for Photovoltaic Applications. *Int. J. Soft Comput. Eng.* **2016**, *6*, 31–37.
42. Saravanan, S.; Babu, N.R. A modified high step-up non-isolated DC–DC converter for PV application. *J. Appl. Res. Technol.* **2017**, *15*, 242–247. [CrossRef]

43. Forouzesh, M.; Siwakoti, Y.P.; Gorji, S.A.; Blaabjerg, F.; Lehman, B. Step-Up DC–DC converters: A comprehensive review of voltage-boosting techniques, topologies, and applications. *IEEE Trans. Power Electron.* **2017**, *32*, 9143–9178. [CrossRef]

44. Huber, L.; Jovanovic, M.M. A design approach for server power supplies for networking applications. In Proceedings of the APEC 2000, Fifteenth Annual IEEE Applied Power Electronics Conference and Exposition (Cat. No.00CH37058), New Orleans, LA, USA, 6–10 February 2000; Volume 2, pp. 1163–1169.

45. Salvador, M.A.; Lazzarin, T.B.; Coelho, R.F. High Step-Up DC–DC Converter with Active Switched-Inductor and Passive Switched-Capacitor Networks. *IEEE Trans. Ind. Electron.* **2018**, *65*, 5644–5654. [CrossRef]

46. Wai, R.-J.; Duan, R.-Y.; Jheng, K.-H. High-efficiency bidirectional DC–DC converter with high-voltage gain. *IET Power Electron.* **2012**, *152*, 793. [CrossRef]

47. Howlader, A.M.; Urasaki, N.; Senjyu, T.; Yona, A.; Saber, A.Y. Optimal PAM control for a buck boost DC–DC converter with a wide-speed-range of operation for a PMSM. *J. Power Electron.* **2010**, *10*, 477–484. [CrossRef]

48. Ned Mohan. *Power Electronics and Drives*; Indian Institute of Technology: Guwahati, India, 2003.

49. Zhang, Y.; Sen, P.C. A new soft-switching technique for buck, boost, and buck–boost converters. *IEEE Trans. Ind. Appl.* **2003**, *39*, 1775–1782. [CrossRef]

50. Lee, Y.J.; Khaligh, A.; Chakraborty, A.; Emadi, A. Digital Combination of Buck and Boost Converters to Control a Positive Buck-Boost Converter and Improve the Output Transients. *IEEE Trans. Power Electron.* **2009**, *24*, 1267–1279. [CrossRef]

51. Gaboriault, M.; Notman, A. A high efficiency, non-inverting, buck–boost DC–DC converter. In Proceedings of the Nineteenth Annual IEEE Applied Power Electronics Conference and Exposition (APEC'04), Anaheim, CA, USA, 22–26 February 2004; Volume 3, pp. 1411–1415.

52. Kang, F.S.; Park, S.J.; Cho, S.E.; Kim, J.M. Photovoltaic power interface circuit incorporated with a buck-boost converter and a full-bridge inverter. *Appl. Energy* **2005**, *82*, 266–283. [CrossRef]

53. Sahu, B.; Rincon-Mora, G.A. A low voltage, dynamic, noninverting, synchronous buck-boost converter for portable applications. *IEEE Trans. Power Electron.* **2004**, *19*, 443–452. [CrossRef]

54. Benavides, N.D.; Chapman, P.L. Power budgeting of a multiple-input buck–boost converter. *IEEE Trans. Power Electron.* **2005**, *20*, 1303–1309. [CrossRef]

55. Ahmed, K.T.; Datta, M.; Mohammad, N. A novel two switch non-inverting buck–boost converter-based maximum power point tracking system. *Int. J. Electron. Comput. Eng.* **2013**, *3*, 467–477.

56. Bose, B.K. Power Electronics, Smart Grid, and Renewable Energy Systems. *Proc. IEEE* **2017**, *105*, 2011–2018. [CrossRef]

57. Chiang, S.J.; Shieh, H.J.; Chen, M.C. Modeling and control of PV charger system with SEPIC converter. *IEEE Trans. Ind. Electron.* **2009**, *56*, 4344–4353. [CrossRef]

58. Niculescu, E.; Marius, C.N.; Dorina, M.P. Modelling the PWM SEPIC converter in discontinuous conduction mode. In Proceedings of the 11th International Conference on Circuits (WSEAS), Crete Island, Greece, 23–25 July 2007.

59. Al-Saffar, M.A.; Ismail, E.H.; Sabzali, A.J.; Fardoun, A.A. An improved topology of SEPIC converter with reduced output voltage ripple. *IEEE Trans. Power Electron.* **2008**, *23*, 2377–2386. [CrossRef]

60. Chen, J.; Chang, C. Analysis and design of SEPIC converter in boundary conduction mode for universal-line power factor correction applications. In Proceedings of the 2001 IEEE 32nd Annual Power Electronics Specialists Conference (IEEE Cat. No.01CH37230), Vancouver, BC, Canada, 17–21 June 2001; Volume 2, pp. 742–747.

61. Mamarelis, E.; Petrone, G.; Spagnuolo, G. Design of a sliding-mode-controlled SEPIC for PV MPPT applications. *IEEE Trans. Ind. Electron.* **2014**, *61*, 3387–3398. [CrossRef]

62. El Khateb, A.; Rahim, N.A.; Selvaraj, J.; Uddin, M.N. Fuzzy-logic-controller-based SEPIC converter for maximum power point tracking. *IEEE Trans. Ind. Appl.* **2014**, *50*, 2349–2358. [CrossRef]

63. Park, H.E.; Song, J.H. A dP/dV feedback-controlled MPPT method for photovoltaic power system using II-SEPIC. *J. Power Electron.* **2009**, *9*, 604–611.

64. Linares-Flores, J.; Sira-Ramírez, H.; Cuevas-López, E.F.; Contreras-Ordaz, M.A. Sensor less passivity-based control of a DC motor via a solar powered sepic converter-full bridge combination. *J. Power Electron.* **2011**, *11*, 743–750. [CrossRef]

65. Kim, I.D.; Kim, J.Y.; Nho, E.C.; Kim, H.G. Analysis and design of a soft-switched PWM Sepic DC–DC converter. *J. Power Electron.* **2010**, *10*, 461–467. [CrossRef]

66. Song, M.S.; Son, Y.D.; Lee, K.H. Non-isolated Bidirectional soft-switching SEPIC/ZETA converter with reduced ripple currents. *J. Power Electron.* **2014**, *14*, 649–660. [CrossRef]

67. Singh, M.D. *Power Electronics*; Tata McGraw-Hill Education: New Delhi, India, 2008.

68. Bist, V.; Singh, B. PFC Cuk converter-fed BLDC motor drive. *IEEE Trans. Power Electron.* **2015**, *30*, 871–887. [CrossRef]

69. Spiazzi, G.; Mattavelli, P. Design criteria for power factor pre regulators based on SEPIC and Cuk converters in continuous conduction mode. In Proceedings of the 1994 IEEE Industry Applications Society Annual Meeting, Denver, CO, USA, 2–6 October 1994.

70. Tse, C.K.; Lai, Y.M.; Lu, H.H.C. Hopf bifurcation and chaos in a free-running current-controlled Ćuk switching regulator. *IEEE Trans. Circuits Syst. I Fundam. Theory Appl.* **2000**, *47*, 448–457. [CrossRef]

71. Moghaddam, A.F.; Van den Bossche, A. A ćuk converter cell balancing technique by using coupled inductors for lithium-based batteries. *Energies* **2019**, *12*, 2881. [CrossRef]

72. Zhu, M.; Luo, F.L. Enhanced self-lift Cûk converter for negative-to-positive voltage conversion. *IEEE Trans. Power Electron.* **2010**, *25*, 2227–2233. [CrossRef]

73. Axelrod, B.; Berkovich, Y.; Tapuchi, S.; Ioinovici, A. Steep Conversion ratio Ćuk, Zeta, and Sepic converters based on a switched coupled-inductor cell. In Proceedings of the 2008 IEEE Power Electronics Specialists Conference, Rhodes, Greece, 15–19 June 2008; pp. 3009–3014.

74. Fardoun, A.A.; Ismail, E.H.; Sabzali, A.J.; Al-Saffar, M.A. New efficient bridgeless cuk rectifiers for PFC applications. *IEEE Trans. Power Electron.* **2012**, *27*, 3292–3301. [CrossRef]

75. Lin, B.R.; Chen, J.J.; Shen, S.F. Zero voltage switching double-ended converter. *IET Power Electron.* **2010**, *57*, 908–912. [CrossRef]

76. Kamnarn, U.; Chunkag, V. Analysis and design of a modular three-phase AC-to-DC converter using CUK rectifier module with nearly unity power factor and fast dynamic response. *IEEE Trans. Power Electron.* **2009**, *24*, 2000–2012. [CrossRef]

77. Darwish, A.; Massoud, A.M.; Holliday, D.; Ahmed, S.; Williams, B.W. Single-Stage Three-Phase Differential-Mode Buck-Boost Inverters with Continuous Input Current for PV Applications. *IEEE Trans. Power Electron.* **2016**, *31*, 8218–8236. [CrossRef]

78. Lee, S.W.; Lee, S.R.; Jeon, C.H. A New High Efficient Bi-directional DC / DC Converter in the Dual Voltage System. *J. Electr. Eng. Technol.* **2006**, *1*, 343–350. [CrossRef]

79. Chen, Z. PI and sliding mode control of a Cuk converter. *IEEE Trans. Power Electron.* **2012**, *27*, 3695–3703. [CrossRef]

80. Elmelegi, A.; Mokhtar Aly; Ahmed, E.M. Developing Phase-Shift PWM-Based Distributed MPPT Technique for Photovoltaic Systems. In Proceedings of the 2019 International Conference on Innovative Trends in Computer Engineering (ITCE'2019), Aswan, Egypt, 2–4 February 2019.

81. Durán, E.; Andújar, J.M.; Segura, F.; Barragán, A.J. A high-flexibility DC load for fuel cell and solar arrays power sources based on DC–DC converters. *Appl. Energy* **2011**, *88*, 1690–1702. [CrossRef]

82. Zhang, M.; Wang, F.; Yang, J.H. Novel Cuk circuit and its application in photovoltaic system. In Proceedings of the 2009 3rd International Conference on Power Electronics Systems and Applications (PESA), Hong Kong, China, 20–22 May 2009.

83. Valencia, P.A.O.; Ramos-Paja, C.A. Sliding-Mode Controller for Maximum Power Point Tracking in Grid-Connected Photovoltaic Systems. *Energies* **2015**, *8*, 12363–12387. [CrossRef]

84. Jiménez-Castillo, G.; Muñoz-Rodríguez, F.J.; Rus-Casas, C.; Gómez-Vidal, P. Improvements in Performance Analysis of Photovoltaic Systems: Array Power Monitoring in Pulse Width Modulation Charge Controllers. *Sensors* **2019**, *19*, 2150. [CrossRef]

85. Tiwari, N.; Bhagwan, D.D. MPPT controller for photo voltaic systems using Cuk DC/DC convertor. *Int. J. Adv. Technol. Eng. Res. (IJATER)* **2012**, *2*, 164–169.

86. Singh, B.; Bist, V.; Chandra, A.; Al-Haddad, K. Power Factor Correction in Bridgeless-Luo Converter-Fed BLDC Motor Drive. *IEEE Trans. Ind. Appl.* **2015**, *51*, 1179–1188. [CrossRef]

87. Lin, L.F.; Ye, H. *Advanced DC/DC Converters*; CRC Press: Boca Raton, FL, USA, 2004.

88. Luo, F.L.; Ye, H. Positive output cascade boost converters. *IEE Proc. Electr. Power Appl.* **2004**, *18*, 105–113. [CrossRef]

89. Manikandan, A.; Vadivel, N. Design and Implementation of Luo Converter for Electric Vehicle Applications. *Int. J. Eng. Trends Technol. (IJETT)* **2013**, *4*, 4437–4441.

90. Luo, F.L.; Ye, H. Hybrid split capacitors and split inductors applied in positive output super-lift Luo-converters. *IET Power Electron.* **2013**, *6*, 1759. [CrossRef]

91. Berkovich, Y.; Axelrod, B.; Madar, R.; Twina, A. Improved Luo converter modifications with increasing voltage ratio. *IET Power Electron.* **2015**, *8*, 202–212. [CrossRef]

92. Ramash Kumar, K.; Jeevananthan, S. Sliding mode control for current distribution control in paralleled positive output Elementary Super Lift Luo converters. *J. Power Electron.* **2011**, *11*, 639–654. [CrossRef]

93. Lai, Y. Introduction to Power Electronics. In Proceedings of the IMID 2009, Seoul, Korea, 12–16 October 2009.

94. Lin, L.F.; Ye, H. *Essential DC/DC Converters*; CRC Press: Boca Raton, FL, USA, 2010.

95. Seyedmahmoudian, M.; Rahmani, R.; Mekhilef, S.; Maung Than Oo, A.; Stojcevski, A.; Soon, T.K.; Ghandhari, A.S. Simulation and Hardware Implementation of New Maximum Power Point Tracking Technique for Partially Shaded PV System Using Hybrid DEPSO Method. *IEEE Trans. Sustain. Energy* **2015**, *6*, 850–862. [CrossRef]

96. Narula, S.; Singh, B.; Bhuvaneswari, G. Power Factor Corrected Welding Power Supply Using Modified Zeta Converter. *IEEE J. Emerg. Sel. Top. Power Electron.* **2016**, *4*, 617–625. [CrossRef]

97. Wu, T.F.; Liang, S.A.; Chen, Y.M. Design optimization for asymmetrical ZVS-PWM Zeta converter. *IEEE Trans. Aerosp. Electron. Syst.* **2003**, *39*, 521–532.

98. Bist, V.; Singh, B. Reduced sensor configuration of brushless DC motor drive using a power factor correction-based modified-zeta converter. *IET Power Electron.* **2014**, *7*, 2322. [CrossRef]

99. Singh, S.; Singh, B.; Bhuvaneswari, G.; Bist, V. Power factor corrected zeta converter based improved power quality switched mode power supply. *IEEE Trans. Ind. Electron.* **2015**, *62*, 5422–5433. [CrossRef]

100. Murthy-Bellur, D.; Kazimierczuk, M.K. Isolated two-transistor zeta converter with reduced transistor voltage stress. *IEEE Trans. Circuits Syst. II Express Briefs* **2011**, *58*, 41–45. [CrossRef]

101. Lin, J.L.; Yang, S.P.; Lin, P.W. Small-signal analysis and controller design for an isolated zeta converter with high power factor correction. *Electr. Power Syst. Res.* **2005**, *76*, 67–76. [CrossRef]

102. Andrade, A.M.S.S.; Beltrame, R.C.; Schuch, L.; Martins, M.L.D.S. PV module-integrated single-switch DC/DC converter for PV energy harvest with battery charge capability. In Proceedings of the 11th IEEE/IAS International Conference on Industry Applications, Juiz de Fora, Brazil, 7–10 December 2014; pp. 1–8.

103. Gules, R.; Dos Santos, W.M.; Dos Reis, F.A.; Romaneli, E.F.R.; Badin, A.A. A modified SEPIC converter with high static gain for renewable applications. *IEEE Trans. Power Electron.* **2014**, *29*, 5860–5871. [CrossRef]

104. Lu, D.D.C.; Agelidis, V.G. Photovoltaic-battery-powered DC bus system for common portable electronic devices. *IEEE Trans. Power Electron.* **2009**, *24*, 849–855. [CrossRef]

105. Sukesh, N.; Pahlevaninezhad, M.; Jain, P.K. Analysis and implementation of a single stage flyback PV microinverter with soft switching. *IEEE Trans. Ind. Electron.* **2014**, *61*, 1819–1833. [CrossRef]

106. Achille, E.; Martiré, T.; Glaize, C.; Joubert, C. Optimized dc-ac boost converters for modular photovoltaic grid-connected generators. In Proceedings of the IEEE International Symposium on Industrial Electronics, Ajaccio, France, 4–7 May 2004; Volume 2, pp. 1005–1010.

107. Hsieh, Y.C.; Chen, M.R.; Cheng, H.L. An interleaved flyback converter featured with zero-voltage transition. *IEEE Trans. Power Electron.* **2011**, *26*, 79–84. [CrossRef]

108. Wu, H.; Chen, R.; Zhang, J.; Xing, Y.; Hu, H.; Ge, H. A family of three-port half-bridge converters for a stand-alone renewable power system. *IEEE Trans. Power Electron.* **2011**, *26*, 2697–2706. [CrossRef]

109. Truong, D.D.; Minh, K.N.; Young, C.L.; Joon, H.C. An Active-Clamped Current-Fed Half-bridge DC–DC Converter with Three Switches. In Proceedings of the International Power Electronics Conference (IPEC-Niigata 2018-ECCE Asia), Niigata, Japan, 20–24 May 2018.

110. Baek, J., II; Kim, C.E.; Kim, K.W.; Lee, M.S.; Moon, G.W. Dual Half-Bridge LLC Resonant Converter with Hybrid-Secondary-Rectifier (HSR) for Wide-Ouput-Voltage Applications. In Proceedings of the 2018 International Power Electronics Conference, IPEC-Niigata-ECCE Asia 2018, Niigata, Japan, 20–24 May 2018; pp. 108–113.

111. Hsieh, H.I.; Chiu, H.L.; Hsieh, G.C. Performance Study of High-Power Half-Bridge Interleaved LLC Converter. In Proceedings of the 2018 International Power Electronics Conference, IPEC-Niigata-ECCE Asia 2018, Niigata, Japan, 20–24 May 2018.

112. Andrijanovitš, A.; Vinnikov, D.; Roasto, I.; Blinov, A. Three-level half-bridge ZVS DC/DC converter for electrolyzer integration with renewable energy systems. In Proceedings of the 10th International Conference on Environment and Electrical Engineering, Rome, Italy, 8–11 May 2011; pp. 1–4.

113. Hu, W.; Wu, H.; Xing, Y.; Sun, K. A full-bridge three-port converter for renewable energy application. In Proceedings of the 2014 IEEE Applied Power Electronics Conference and Exposition-APEC 2014, Fort Worth, TX, USA, 16–20 March 2014.

114. Cha, W.J.; Kwon, J.M.; Kwon, B.H. Highly Efficient Asymmetrical PWM Full-Bridge Converter for Renewable Energy Sources. *IEEE Trans. Ind. Electron.* **2016**, *63*, 2945–2953. [CrossRef]

115. Patil, U.; Nagendrappa, H. Analysis and design of a high frequency isolated full bridge CLL resonant DC–DC converter for renewable energy applications. In Proceedings of the 2018 IEEE International Conference on Power, Instrumentation, Control and Computing (PICC 2018), Thrissur, India, 18–20 January 2018.

116. Sathishkumar, P.; Himanshu; Piao, S.; Adil Khan, M.; Kim, D.H.; Kim, M.S.; Jeong, D.K.; Lee, C.; Kim, H.J. A blended SPS-ESPS control DAB-IBDC converter for a standalone solar power system. *Energies* **2017**, *10*, 1431. [CrossRef]

117. Jeong, D.K.; Kim, H.S.; Baek, J.W.; Kim, J.Y.; Kim, H.J. Dual active bridge converter for Energy Storage System in DC microgrid. In Proceedings of the 2016 IEEE Transportation Electrification Conference and Expo, Asia-Pacific (ITEC Asia-Pacific 2016), Busan, Korea, 1–4 June 2016.

118. Stieneker, M.; De Doncker, R.W. Dual-active bridge DC–DC converter systems for medium-voltage DC distribution grids. In Proceedings of the 2015 IEEE 13th Brazilian Power Electronics Conference and 1st Southern Power Electronics Conference (COBEP/SPEC 2016), Fortaleza, Brazil, 29 November–2 December 2015.

119. Ryu, M.; Jung, D.; Baek, J.; Kim, H. An optimized design of bi-directional dual active bridge converter for low voltage battery charger. In Proceedings of the 16th International Power Electronics and Motion Control Conference and Exposition (PEMC 2014_, Antalya, Turkey, 21–24 September 2014.

120. Naayagi, R.T.; Forsyth, A.J.; Shuttleworth, R. High-power bidirectional DC–DC converter for aerospace applications. *IEEE Trans. Power Electron.* **2012**, *27*, 4366–4379. [CrossRef]

121. Zhao, B.; Song, Q.; Liu, W.; Sun, Y. Overview of dual-active-bridge isolated bidirectional DC–DC converter for high-frequency-link power-conversion system. *IEEE Trans. Power Electron.* **2014**, *29*, 4091–4106. [CrossRef]

122. Zhou, H.; Khambadkone, A.M. Hybrid modulation for dual-active-bridge bidirectional converter with extended power range for ultracapacitor application. *IEEE Trans. Ind. Appl.* **2009**, *45*, 1434–1442. [CrossRef]

123. Sathishkumar, P.; Krishna, T.N.V.; Himanshu; Khan, M.A.; Zeb, K.; Kim, H.J. Digital soft start implementation for minimizing start up transients in high power DAB-IBDC converter. *Energies* **2018**, *11*, 956. [CrossRef]

124. Rodríguez, A.; Vázquez, A.; Lamar, D.G.; Hernando, M.M.; Sebastián, J. Different purpose design strategies and techniques to improve the performance of a dual active bridge with phase-shift control. *IEEE Trans. Power Electron.* **2015**, *30*, 790–804. [CrossRef]

125. Khodabakhsh, J.; Moschopoulos, G. A study of multilevel resonant DC–DC converters for conventional DC voltage bus applications. In Proceedings of the Conference on IEEE Applied Power Electronics Conference and Exposition (APEC), San Antonio, TX, USA, 4–8 March 2018.

126. Deng, J.; Li, S.; Hu, S.; Mi, C.C.; Ma, R. Design methodology of LLC resonant converters for electric vehicle battery chargers. *IEEE Trans. Veh. Technol.* **2014**, *63*, 1581–1592. [CrossRef]

127. Jabbari, M.; Kazemi, H.; Hematian, N.; Shahgholian, G. A novel resonant LLC soft-switching buck converter. In Proceedings of the IEEE International Symposium on Industrial Electronics, Istanbul, Turkey, 1–4 June 2014.

128. Sharifi, S.; Jabbari, M. Farzanehfard, H. A New Family of Single-Switch ZVS Resonant Converters. *IEEE Trans. Ind. Electron.* **2017**. [CrossRef]

129. Mishima, T.; Nakaoka, M. A new family of 2ZCS-PWM DC–DC converters with clamping diodes-assisted active edge-resonant cell. In Proceedings of the 2010 International Conference on Electrical Machines and Systems (ICEMS 2010), Incheon, Korea, 10–13 October 2010.

130. Huang, D.; Lee, F.C.; Fu, D. Classification and selection methodology for multi-element resonant converters. In Proceedings of the Conference on IEEE Applied Power Electronics Conference and Exposition (APEC), Fort Worth, TX, USA, 6–11 March 2011.

131. Huang, D.; Kong, P.; Lee, F.C.; Fu, D. A novel integrated multi-elements resonant converter. In Proceedings of the IEEE Energy Conversion Congress and Exposition: Energy Conversion Innovation for a Clean Energy Future (ECCE 2011), Proceedings, Phoenix, AZ, USA, 17–22 September 2011.

132. Chen, Y.; Wang, H.; Liu, Y.F.; Afsharian, J.; Yang, Z.A. Efficiency-wise optimal design methodology of LCLC converter for wide input voltage range applications. In Proceedings of the 2016 IEEE Energy Conversion Congress and Exposition (ECCE), Milwaukee, WI, USA, 18–22 September 2016.

133. Fu, D.; Lee, F.C.; Liu, Y.; Xu, M. Novel Multi-element resonant converters for front-end DC/DC converters. In Proceedings of the 2008 IEEE Power Electronics Specialists Conference, Rhodes, Greece, 15–19 June 2008; pp. 358–364.

134. Wu, H.; Jin, X.; Hu, H.; Xing, Y. Multielement Resonant Converters with a Notch Filter on Secondary Side. *IEEE Trans. Power Electron.* **2016**, *31*, 3999–4004. [CrossRef]

135. Mizutani, H.; Mishima, T.; Nakaoka, M. A dual pulse modulated five-element multi-resonant DC–DC converter and its performance evaluations. In Proceedings of the 2013 IEEE Energy Conversion Congress and Exposition (ECCE 2013), Denver, CO, USA, 15–19 September 2013.

136. Wang, Y.; Han, F.; Yang, L.; Xu, R.; Liu, R. A Three-Port Bidirectional Multi-Element Resonant Converter with Decoupled Power Flow Management for Hybrid Energy Storage Systems. *IEEE Access* **2018**, *6*, 61331–61341. [CrossRef]

137. Petit, P.; Aillerie, M.; Sawicki, J.P.; Charles, J.P. Push-pull converter for high efficiency photovoltaic conversion. *Energy Procedia* **2012**, *18*, 1583–1592. [CrossRef]

138. Zhang, M.T.; Jovanovic, M.M.; Lee, F.C. Analysis, design, and evaluation of forward converter with distributed magnetics-interleaving and transformer paralleling. In Proceedings of the Conference on IEEE Applied Power Electronics Conference and Exposition (APEC), Dallas, TX, USA, 5–9 March 1995.

139. Islam, S.U.; Zeb, K.; Din, W.U.; Khan, I.; Ishfaq, M.; Hussain, A.; Busarello, T.D.C.; Kim, H.J. Design of Robust Fuzzy Logic Controller Based on the Levenberg Marquardt Algorithm and Fault Ride Trough Strategies for a Grid-Connected PV System. *Electronics* **2019**, *8*, 429. [CrossRef]

140. Dasgupta, N.; Pandey, A.; Mukerjee, A.K. Voltage-sensing-based photovoltaic MPPT with improved tracking and drift avoidance capabilities. *Sol. Energy Mater. Sol. Cells* **2008**, *92*, 1552–1558. [CrossRef]

141. Salas, V.; Olías, E.; Lázaro, A.; Barrado, A. Evaluation of a new maximum power point tracker (MPPT) applied to the photovoltaic stand-alone systems. *Sol. Energy Mater. Sol. Cells* **2005**, *87*, 807–815. [CrossRef]

142. Kawamura, T.; Harada, K.; Ishihara, Y.; Todaka, T.; Oshiro, T.; Nakamura, H.; Imataki, M. Analysis of MPPT characteristics in photovoltaic power system. *Sol. Energy Mater. Sol. Cells* **1997**, *47*, 155–165. [CrossRef]

143. Muhidaa, R.; Park, M.; Mohammed, D.; Kenji, M.; Akira, T.; Masakazu, M. A maximum power point tracking for photovoltaic-SPE system using a maximum current controller. *Sol. Energy Mater. Sol. Cells* **2003**, *75*, 697–706. [CrossRef]

144. Kobayashi, K.; Takano, I.; Sawada, Y. A study of a two-stage maximum power point tracking control of a photovoltaic system under partially shaded insolation conditions. *Sol. Energy Mater. Sol. Cells.* **2006**, *90*, 2975–2988. [CrossRef]

145. Matsukawa, H.; Koshiishi, K.; Koizumi, H.; Kurokawa, K.; Hamada, M.; Bo, L. Dynamic evaluation of maximum power point tracking operation with PV array simulator. *Sol. Energy Mater. Sol. Cells.* **2003**, *75*, 537–546. [CrossRef]

146. Salas, V.; Olías, E.; Lázaro, A.; Barrado, A. New algorithm using only one variable measurement applied to a maximum power point tracker. *Sol. Energy Mater. Sol. Cells* **2005**, *87*, 675–684. [CrossRef]

147. Muñoz, F.J.; Almonacid, G.; Nofuentes, G.; Almonacid, F. A new method based on charge parameters to analyse the performance of stand-alone photovoltaic systems. *Sol. Energy Mater. Sol. Cells* **2006**, *90*, 1750–1763. [CrossRef]

148. Roy Chowdhury, S.; Saha, H. Maximum power point tracking of partially shaded solar photovoltaic arrays. *Sol. Energy Mater. Sol. Cells* **2010**, *94*, 1441–1447. [CrossRef]

149. Giustiniani, A.; Petrone, G.; Spagnuolo, G.; Vitelli, M. Low-frequency current oscillations and maximum power point tracking in grid-connected fuel-cell-based systems. *IEEE Trans. Ind. Electron.* **2010**, *57*, 2042–2053. [CrossRef]

150. Noguchi, T.; Togashi, S.; Nakamoto, R. Short-current pulse-based maximum-power-point tracking method for multiple photovoltaic-and-converter module system. *IEEE Trans. Ind. Electron.* **2002**, *49*, 217–223. [CrossRef]

151. Xiao, W.; Dunford, W.G.; Palmer, P.R.; Capel, A. Application of centered differentiation and steepest descent to maximum power point tracking. *IEEE Trans. Ind. Electron.* **2007**, *54*, 2539–2549. [CrossRef]

152. Baimel, D.; Tapuchi, S.; Levron, Y.; Belikov, J. Improved Fractional Open Circuit Voltage MPPT Methods for PV Systems. *Electronics* **2019**, *8*, 321. [CrossRef]

153. Ahmad, J. A fractional open circuit voltage based maximum power point tracker for photovoltaic arrays. In Proceedings of the ICSTE 2010 2nd International Conference on Software Technology and Engineering, San Juan, PR, USA, 3–5 October 2010; pp. 247–250.

154. Masoum, M.A.S.; Dehbonei, H.; Fuchs, E.F. Theoretical and experimental analyses of photovoltaic systems with voltage- and current-based maximum power-point tracking. *IEEE Trans. Energy Convers.* **2002**, *17*, 514–522. [CrossRef]

155. Veerachary, M.; Senjyu, T.; Uezato, K. Voltage-based maximum power point tracking control of PV system. *IEEE Trans. Aerosp. Electron. Syst.* **2002**, *38*, 262–270. [CrossRef]

156. Esram, T.; Kimball, J.W.; Krein, P.T.; Chapman, P.L.; Midya, P. Dynamic maximum power point tracking of photovoltaic arrays using ripple correlation control. *IEEE Trans. Power Electron.* **2006**, *21*, 1282–1291. [CrossRef]

157. Kimball, J.W.; Krein, P.T. Discrete-time ripple correlation control for maximum power point tracking. *IEEE Trans. Power Electron.* **2008**, *23*, 2353–2362. [CrossRef]

158. Casadei, D.; Grandi, G.; Rossi, C. Single-phase single-stage photovoltaic generation system based on a ripple correlation control maximum power point tracking. *IEEE Trans. Energy Convers.* **2006**, *21*, 562–568. [CrossRef]

159. Serna-Garcés, S.I.; Montoya, D.G.; Ramos-Paja, C.A. Sliding-mode control of a charger/discharger DC/DC converter for DC-bus regulation in renewable power systems. *Energies* **2016**, *9*, 245. [CrossRef]

160. Kim, I.S.; Kim, M.B.; Youn, M.J. New maximum power point tracker using sliding-mode observer for estimation of solar array current in the grid-connected photovoltaic system. *IEEE Trans. Ind. Electron.* **2006**, *53*, 1027–1035. [CrossRef]

161. Aghatehrani, R.; Kavasseri, R. Sensitivity-analysis-based sliding mode control for voltage regulation in microgrids. *IEEE Trans. Sustain. Energy* **2013**, *4*, 50–57. [CrossRef]

162. Quamruzzaman, M.; Rahman, K.M. A modified Perturb and observe maximum power point tracking technique for single-stage grid-connected photovoltaic inverter. *WSEAS Trans. Power Syst.* **2014**, *9*, 111–118.

163. Femia, N.; Petrone, G.; Spagnuolo, G.; Vitelli, M. Increasing the efficiency of P&O MPPPT by converter dynamic matching. In Proceedings of the IEEE International Symposium on Industrial Electronics, Ajaccio, France, 4–7 May 2004; Volume 2, pp. 1017–1021.

164. Jung, Y.; Therefore, J.; Yu, G.; Choi, J. Improved perturbation and observation method (IP&O) of MPPT control for photovoltaic power systems. In Proceedings of the Conference Record of the IEEE Photovoltaic Specialists Conference, Lake Buena Vista, FL, USA, 3–7 January 2005.

165. Liu, X.; Lopes, L.A.C. An improved perturbation and observation maximum power point tracking algorithm for PV arrays. In Proceedings of the 2004 35th IEEE Annual Power Electronics Specialists Conference (IEEE Cat. No.04CH37551), Aachen, Germany, 20–25 June 2004; Volume 3, pp. 2005–2010.

166. Ishaque, K.; Salam, Z.; Lauss, G. The performance of perturb and observe and incremental conductance maximum power point tracking method under dynamic weather conditions. *Appl. Energy* **2014**, *119*, 228–236. [CrossRef]

167. Tey, K.S.; Mekhilef, S. Modified incremental conductance MPPT algorithm to mitigate inaccurate responses under fast-changing solar irradiation level. *Sol. Energy* **2014**, *101*, 333–342. [CrossRef]

168. Radjai, T.; Rahmani, L.; Mekhilef, S.; Gaubert, J.P. Implementation of a modified incremental conductance MPPT algorithm with direct control based on a fuzzy duty cycle change estimator using dSPACE. *Sol. Energy* **2014**, *110*, 325–337. [CrossRef]

169. Putri, R.I.; Wibowo, S.; Rifa'i, M. Maximum power point tracking for photovoltaic using incremental conductance method. *Energy Procedia* **2015**, *88*, 4840–4847. [CrossRef]

170. Sivakumar, P.; Abdul Kader, A.; Kaliavaradhan, Y.; Arutchelvi, M. Analysis and enhancement of PV efficiency with incremental conductance MPPT technique under non-linear loading conditions. *Renew. Energy* **2015**, *81*, 543–550. [CrossRef]

171. Carrasco, J.M.; Franquelo, L.G.; Bialasiewicz, J.T.; Galván, E.; Portillo Guisado, R.C.; Prats, M.Á.M.; León, J.I.; Moreno-Alfonso, N. Power-electronic systems for the grid integration of renewable energy sources: A survey. *IEEE Trans. Ind. Electron.* **2006**, *53*, 1002–1016. [CrossRef]

172. Patcharaprakiti, N.; Premrudeepreechacharn, S.; Sriuthaisiriwong, Y. Maximum power point tracking using adaptive fuzzy logic control for grid-connected photovoltaic system. *Renew. Energy* **2005**, *30*, 1771–1788. [CrossRef]

173. Veerachary, M.; Senjyu, T.; Uezato, K. Feedforward maximum power point tracking of PV systems using fuzzy controller. *IEEE Trans. Aerosp. Electron. Syst.* **2002**, *38*, 969–981. [CrossRef]

174. Chiu, C.S. T-S fuzzy maximum power point tracking control of solar power generation systems. *IEEE Trans. Energy Convers.* **2010**, *25*, 1123–1132. [CrossRef]

175. Nabulsi, A.A.; Dhaouadi, R.; Rehman, H.U. Single input fuzzy controller (SFLC)-based maximum power point tracking. In Proceedings of the 2011 4th International Conference on Modeling, Simulation and Applied Optimization (ICMSAO 2011), Kuala Lumpur, Malaysia, 19–21 April 2011; pp. 1–5.

176. Algazar, M.M.; Al-Monier, H.; El-Halim, H.A.; Salem, M.E.E.K. Maximum power point tracking using fuzzy logic control. *Int. J. Electr. Power Energy Syst.* **2012**, *39*, 21–28. [CrossRef]

177. Ibrahim, H.E.A.; Ibrahim, M. Comparison Between Fuzzy and P&O Control for MPPT for Photovoltaic System Using Boost Converter. *J. Energy Technol. Policy* **2012**, *2*, 1–12.

178. Veerachary, M.; Senjyu, T.; Uezato, K. Neural-network-based maximum-power-point tracking of coupled-inductor interleaved-boost-converter-supplied PV system using fuzzy controller. *IEEE Trans. Ind. Elec.* **2003**, *50*, 749–758. [CrossRef]

179. Rizzo, S.A.; Scelba, G. ANN based MPPT method for rapidly variable shading conditions. *Appl. Energy* **2015**, *145*, 124–132. [CrossRef]

180. Younis, M.A.; Najeeb, M.; Mohd Ariffin, A.; Khatib, T. An improved maximum power point tracking controller for PV systems using artificial neural network. *Prz. Elektrotech.* **2012**, *88*, 116–121.

181. Asiful Islam, M.; Ashfanoor Kabir, M. Neural network-based maximum power point tracking of photovoltaic arrays. In Proceedings of the IEEE Region 10 Annual International Conference (TENCON 2011), Bali, Indonesia, 21–24 November 2011; pp. 79–82.

182. Ramaprabha, R.; Mathur, B.L. Intelligent Controller-based Maximum Power Point Tracking for Solar PV System. *Int. J. Comput. Appl.* **2011**, *12*, 37–41. [CrossRef]

183. Bendib, B.; Krim, F.; Belmili, H.; Almi, M.F.; Boulouma, S. Advanced fuzzy MPPT controller for a stand-alone PV system. *Energy Procedia* **2014**, *50*, 383–392. [CrossRef]

184. Alabedin, A.M.Z.; El-Saadany, E.F.; Salama, M.M.A. Maximum power point tracking for Photovoltaic systems using fuzzy logic and artificial neural networks. In Proceedings of the IEEE Power and Energy Society General Meeting, Detroit, MI, USA, 24–28 July 2011; pp. 1–9.

185. Radhakrishnan, S.; Venugopal, L.V.; Vanitha, M. Hardware implimentation of linear current booster for solar pumping applications. *ARPN J. Eng. Appl. Sci.* **2016**, *11*, 1124–1126.

186. Zhang, L.; Hurley, W.G.; Wölfle, W.H. A new approach to achieve maximum power point tracking for PV system with a variable inductor. *IEEE Trans. Power Electron.* **2011**, *26*, 948–952. [CrossRef]

187. Veerachary, M. Fourth-order buck converter for maximum power point tracking applications. *IEEE Trans. Aerosp. Electron. Syst.* **2011**, *47*, 896–911. [CrossRef]

188. Kwon, J.M.; Kwon, B.H.; Nam, K.H. Three-phase photovoltaic system with three-level boosting MPPT control. *IEEE Trans. Power Electron.* **2008**, *23*, 2319–2327. [CrossRef]

189. Choi, S.; Agelidis, V.G.; Yang, J.; Coutellier, D.; Marabeas, P. Analysis, design and experimental results of a floating-output interleaved-input boost-derived DC–DC high-gain transformer-less converter. *IET Power Electron.* **2011**, *4*, 168–180. [CrossRef]

190. Elshaer, M.; Mohamed, A.; Mohammed, O. Smart optimal control of DC–DC boost converter in PV systems. In Proceedings of the 2010 IEEE/PES Transmission and Distribution Conference and Exposition: Latin America (T&D-LA), Hersonissos, Greece, 25–28 September 2011; pp. 403–410.

191. Agorreta, J.L.; Reinaldos, L.; González, R.; Borrega, M.; Balda, J.; Marroyo, L. Fuzzy switching technique applied to PWM boost converter operating in mixed conduction mode for PV systems. *IEEE Trans. Ind. Electron.* **2009**, *56*, 4363–4373. [CrossRef]

192. Ishaque, K.; Salam, Z.; Amjad, M.; Mekhilef, S. An improved particle swarm optimization (PSO)-based MPPT for PV with reduced steady-state oscillation. *IEEE Trans. Power Electron.* **2012**, *27*, 3627–3638. [CrossRef]

193. Wu, T.F.; Yang, C.H.; Chen, Y.K.; Liu, Z.R. Photovolatic inverter systems with self-tuning fuzzy control based on an experimental planning method. In Proceedings of the Conference Record of the 1999 IEEE Industry Applications Conference, Thirty-Forth IAS Annual Meeting (Cat. No.99CH36370), Phoenix, AZ, USA, 3–7 October 1999.

194. Miyatake, M.; Veerachary, M.; Toriumi, F.; Fujii, N.; Ko, H. Maximum power point tracking of multiple photovoltaic arrays: A PSO approach. *IEEE Trans. Aerosp. Electron. Syst.* **2011**, *47*, 367–380. [CrossRef]

195. Syafaruddin; Karatepe, E.; Hiyama, T. Artificial neural network-polar coordinated fuzzy controller-based maximum power point tracking control under partially shaded conditions. *IET Renew. Power Gener.* **2009**, *3*, 239–253. [CrossRef]

196. Kuo, J.L.; Chao, K.L.; Lee, L.S. Dual mechatronic MPPT controllers with PN and OPSO control algorithms for the rotatable solar panel in PHEV system. *IEEE Trans. Ind. Electron.* **2010**, *57*, 678–689.

197. Lin, B.R.; Huang, C.L.; Tsao, F.P. Integrated Cuk-forward converter for photovoltaic-based LED lighting. *Int. J. Electron.* **2009**, *96*, 943–959. [CrossRef]

198. Chung, H.S.H.; Tse, K.K.; Ron Hui, S.Y.; Mok, C.M.; Ho, M.T. A novel maximum power point tracking technique for solar panels using a SEPIC or Cuk converter. *IEEE Trans. Power Electron.* **2003**, *18*, 717–724. [CrossRef]

199. Mahmoud, A.M.A.; Mashaly, H.M.; Kandil, S.A.; El Khashab, H.; Nashed, M.N.F. Fuzzy logic implementation for photovoltaic maximum power tracking. In Proceedings of the 2000 26th Annual Conference of the IEEE Industrial Electronics Society (IECON 2000), Nagoya, Japan, 22–28 October 2000; Volume 1, pp. 735–740.

200. Safari, A.; Mekhilef, S. Simulation and hardware implementation of incremental conductance MPPT with direct control method using cuk converter. *IEEE Trans. Ind. Electron.* **2011**, *58*, 1154–1161. [CrossRef]

201. Durán, E.; Andújar, J.M.; Galán, J.; Sidrach-De-Cardona, M. Methodology and experimental system for measuring and displaying I-V characteristic curves of PV facilities. *Prog. Photovolt. Res. Appl.* **2009**, *17*, 574–586. [CrossRef]

202. Tse, K.K.; Ho, M.T.; Chung, H.S.H.; Hui, S.Y.R. A novel maximum power point tracker for PV panels using switching frequency modulation. *IEEE Trans. Power Electron.* **2002**, *17*, 980–989. [CrossRef]

203. Do, H.L. Soft-switching SEPIC converter with ripple-free input current. *IEEE Trans. Power Electron.* **2012**, *27*, 2879–2887. [CrossRef]

204. Rathge, C.; Mecke, R. Converter for energy storage integration in photovoltaic plants. In Proceedings of the 2002 IEEE International Symposium on Industrial Electronics, L'Aquila, Italy, 8–11 July 2002; Volume 3, pp. 959–963.

205. Salenga, J.S.; Magsino, E.R. Dynamic analysis of a two-input Zeta converter topology for modular hybrid PV-wind microgrid system. In Proceedings of the IEEE Region 10 Annual International Conference, Proceedings (TENCON 2015), Macao, China, 1–4 November 2015; pp. 1–6.

206. Sivasakthi Priya, R.; Inayath Bathul, I. Adaptive P & O MPPT method using zeta converter for solar PV systems. *Int. J. Res. Appl. Sci. Eng. Technol. (IJRASET)* **2016**, *4*, 215–220.

207. Andrade, A.M.S.S.; Schuch, L.; Martins, M.L.D.S. Photovoltaic battery charger based on the Zeta converter: Analysis, design and experimental results. In Proceedings of the IEEE International Symposium on Industrial Electronics, Buzios, Brazil, 3–5 June 2015; pp. 379–384.

208. Zanotti, J.W.; Martins, D.C. Input characteristic impedance technique of power converters circuits applied to the maximum power point tracker of photovoltaic panels. In Proceedings of the IEEE Asia-Pacific Conference on Circuits and Systems (APCCAS), Ishigaki, Japan, 17–20 November 2014; pp. 292–295.

209. Yilmaz, U.; Kircay, A.; Borekci, S. PV system fuzzy logic MPPT method and PI control as a charge controller. *Renew. Sustain. Energy Rev.* **2018**, *81*, 994–1001. [CrossRef]

210. Shanmugavel, D.; Kalaiselvi, M.; Mohanram, S.; Kalidasan, M. International Journal of Advanced Research in Electrical. *Electron. Instrum. Eng.* **2016**, *5*, 109–116.

211. Ryu, D.K.; Choi, B.Y.; Lee, S.R.; Kim, Y.H.; Won, C.Y. Flyback inverter using voltage sensor less MPPT for photovoltaic AC modules. *J. Power Electron.* **2014**, *14*, 1293–1302. [CrossRef]

212. Ashiqah, P.K.M.; Maheswari, M. Modified MPPT controlled PV with flyback converter for AC load applications. *Int. J. Appl. Eng. Res.* **2015**, *10*, 18826–18830.

213. Ramos-Paja, C.A.; Montoya, D.G.; Bastidas-Rodriguez, J.D. Sliding-mode control of distributed maximum power point tracking converters featuring overvoltage protection. *Energies* **2018**, *11*, 2220. [CrossRef]

214. Mustafa, E.B. Forward Converter Based Distributed Maximum Power Point Tracking. In Proceedings of the 5th International Conference on Engineering Sciences, Ankara, Turkey, 19 September 2019; pp. 1–5.

215. Loukriz, A.; Messalti, S.; Harrag, A. Design, simulation, and hardware implementation of novel optimum operating point tracker of PV system using adaptive step size. *Int. J. Adv. Manuf. Technol.* **2019**, *101*, 1671–1680. [CrossRef]

216. Karafil, A.; Ozbay, H.; Oncu, S. Power control of resonant converter MPPT by pulse density modulation. In Proceedings of the 2017 10th International Conference on Electrical and Electronics Engineering (ELECO), Bursa, Turkey, 30 November–2 December 2017; pp. 360–364.

217. Meghana, M.N.; Naveenkumar, S.B. MPPT based LLC resonant converter for PV applications. In Proceedings of the 6th International Conference on Computation of Power, Energy, Information and Communication (ICCPEIC 2017), Melmaruvathur, India, 22–23 March 2017.

218. Adrian, S.T.T.; Shahid, I.; Ishak, D. LLC Resonant Converter Based Incremental Conductance Maximum Power Point Tracking System for PV Applications. In Proceedings of the 9th International Conference on Robotic, Vision, Signal Processing and Power Applications, Singapore, 29 September 2016.

219. Zhang, Q.; Batarseh, I.; Chen, L. Variable Frequency Iteration MPPT for Resonant Power Converters. UCF Patents 637, 30 June 2015.

220. Piegari, L.; Rizzo, R.; Spina, I.; Tricoli, P. Optimized adaptive perturb and observe maximum power point tracking control for photovoltaic generation. *Energies* **2015**, *8*, 3418–3436. [CrossRef]

221. Gaikwad, D.D.; Chavan, M.S.; Gaikwad, M.S. Hardware implementation of DC–DC converter for MPPT in PV applications. In Proceedings of the on 2014 IEEE Global Conference on Wireless Computing and Networking (GCWCN 2014), Lonavala, India, 22–24 December 2014; pp. 16–20.

222. Piegari, L.; Rizzo, R. Adaptive perturb and observe algorithm for photovoltaic maximum power point tracking. *IET Renew. Power Gener.* **2010**, *4*, 317–328. [CrossRef]

223. Mahraz, A.; Hossein, I. A Modified Maximum Power Point Tracking Technique for Grid Connected Cascaded H Bridge Photovoltaic Inverter Under Partial Shading Conditions. *Int. Res. J. Eng. Technol.* **2018**, *5*, 514–522.

224. Xiao, B.; Shen, K.; Mei, J.; Filho, F.; Tolbert, L.M. Control of cascaded H-bridge multilevel inverter with individual MPPT for grid-connected photovoltaic generators. In Proceedings of the 2012 IEEE Energy Conversion Congress and Exposition (ECCE 2012), Raleigh, NC, USA, 15–20 September 2012.

225. Natasha, N.I.; Bhuiyan, W.T.; Razzak, M.A. Implementation of Maximum Power Point Tracking in a photovoltaic inverter using Incremental Conductance technique. In Proceedings of the 8th International Conference on Electrical and Computer Engineering, Dhaka, Bangladesh, 20–22 December 2014; pp. 329–332.

226. Mao, M.; Zhang, L.; Duan, Q.; Chong, B. Multilevel DC-link converter photovoltaic system with modified PSO based on maximum power point tracking. *Sol. Energy* **2017**, *153*, 329–342. [CrossRef]

227. Rejas, M.; Mathe, L.; Dan Burlacu, P.; Pereira, H.; Sangwongwanich, A.; Bongiorno, M.; Teodorescu, R. Performance comparison of phase shifted PWM and sorting method for modular multilevel converters. In Proceedings of the 2015 17th European Conference on Power Electronics and Applications (EPE-ECCE Europe 2015), Geneva, Switzerland, 8–10 September 2015; pp. 1–10.

228. Chen, Y.M.; Chen, Y.C.; Wu, H.C.; Chen, T.M. An improved delta modulation technique for DC–DC buck converters. In Proceedings of the 2008 IEEE International Conference on Sustainable Energy Technologies (ICSET 2008), Singapore, 24–27 November 2008; pp. 496–501.

229. Mandi, B.C.; Kapat, S.; Patra, A. Unified Digital Modulation Techniques for DC–DC Converters over a Wide Operating Range: Implementation, Modeling, and Design Guidelines. *IEEE Trans. Circuits Syst. I Regul. Pap.* **2018**, *65*, 1442–1453. [CrossRef]

230. Boudouda, A.; Boudjerda, N.; Aibeche, A.; Bouzida, A. Dual randomized pulse width modulation technique for buck converter fed by photovoltaic source. *Rev. Roum. Sci. Tech. Ser. Électrotech. Énerg.* **2018**, *63*, 289–294.

231. Nguyen, V.H.; Huynh, H.A.; Kim, S.; Song, H. Active EMI reduction using chaotic modulation in a buck converter with relaxed output LC filter. *Electronics* **2018**, *7*, 254. [CrossRef]

232. Diab, M.S.; Elserougi, A.; Abdel-Khalik, A.S.; Massoud, A.M.; Ahmed, S. Modified modulation scheme for photovoltaic fed grid-connected three-phase boost inverter. In Proceedings of the 39th Annual Conference of the IEEE Industrial Electronics Society (IECON 2013), Vienna, Austria, 10–13 November 2013; pp. 1735–1740.

233. Parveen, N.; Rupesh, K.C. Design and simulation of interleaved DC–DC boost converter for three-phase loads using solar panel. In Proceedings of the 2016 International Conference on Computation of Power, Energy, Information and Communication (ICCPEIC 2016), Chennai, India, 20–21 April 2016; pp. 514–519.

234. Morrison, R.; Egan, M.G. A new modulation strategy for a buck–boost input AC/DC converter. *IEEE Trans. Power Electron.* **2001**, *16*, 34–45. [CrossRef]

235. Waffler, S.; Kolar, J.W. A Novel Low-Loss Modulation Strategy for High-Power Bidirectional Buck + Boost Converters. *IEEE Trans. Power Electron.* **2009**, *24*, 1589–1599. [CrossRef]

236. Li, N. Digital Control Strategies for DC/DC SEPIC Converters towards Integration. Ph.D. Thesis, INSA de Lyon, Lyon, France, 2012.

237. Mohanraj, K.; Kiran, Y.B. PV Integrated SEPIC Converter Using Maximum Power Point Tracking for Ac Loads. *Int. J. Recent Technol. Eng.* **2019**, *8*, 565–570.

238. Ozsoy, E.; Padmanaban, S.; Blaabjerg, F.; Ionel, D.M.; Kalla, U.K.; Bhaskar, M.S. Control of High Gain Modified SEPIC Converter: A Constant Switching Frequency Modulation Sliding Mode Controlling Technique. In Proceedings of the on 2018 IEEE International Power Electronics and Application Conference and Exposition (PEAC 2018), Shenzhen, China, 4–7 November 2018.

239. Ruseler, A.; Barbi, I. Isolated Zeta-SEPIC bidirectional DC–DC converter with active-clamping. In Proceedings of the 2013 Brazilian Power Electronics Conference, Gramado, Brazil, 27–31 October 2013; pp. 123–128.

240. Bawane, B.R. A Study on SEPIC Converter for Voltage Modification Fed by Solar Photovoltaic Systems. In Proceedings of the 7th IEEE International Conference on Computation of Power, Energy, Information and Communication (ICCPEIC 2018), Chennai, India, 28–29 March 2018; pp. 243–247.

241. Hu, J.; Sagneri, A.D.; Rivas, J.M.; Han, Y.; Davis, S.M.; Perreault, D.J. High-frequency resonant SEPIC converter with wide input and output voltage ranges. *IEEE Trans. Power Electron.* **2012**, *27*, 189–200. [CrossRef]

242. Gao, F.; Loh, P.C.; Teodorescu, R.; Blaabjerg, F.; Vilathgamuwa, D.M. Topological design and modulation strategy for buck–boost three-level inverters. *IEEE Trans. Power Electron.* **2009**, *24*, 1578–1584. [CrossRef]

243. Ragavendra, B.; Vijayanand, S.; Jayaprakash, B. Improved Control Strategy on Cuk Converter fed DC Motor using Artificial Bee Colony Algorithm. *Int. J. Recent Dev. Eng. Technol.* **2014**, *2*, 181–188.

244. Krishnakumar, C.; Muhilan, P.; Sathiskumar, M.; Sakthivel, M. A New Random PWM technique for conducted-EMI mitigation on Cuk Converter. *J. Electr. Eng. Technol.* **2015**, *10*, 916–924. [CrossRef]

245. Fuad, Y.; de Koning, W.L.; van der Woude, J.W. On the Stability of the Pulsewidth-Modulated Ćuk Converter. *IEEE Trans. Circuits Syst. II Express Briefs* **2004**, *51*, 412–420. [CrossRef]

246. Mehrnami, S.; Mazumder, S.K.; Soni, H. Modulation scheme for three-phase differential-mode ćUK inverter. *IEEE Trans. Power Electron.* **2016**, *31*, 1–15. [CrossRef]

247. Lessing, M.H.; Agostini, E.; Barbi, I. An improved modulation strategy for the high-frequency-isolated DC-AC flyback converter with differential output connection. In Proceedings of the 2016 12th IEEE International Conference on Industry Applications (INDUSCON 2016), Curitiba, Brazil, 20–23 November 2016; pp. 1–7.

248. Sable, D.M.; Cho, B.H.; Ridley, R.B. Use of Leading-Edge Modulation to Transform Boost and Flyback Converters into Minimum-Phase-Zero Systems. *IEEE Trans. Power Electron.* **1991**, *6*, 704–711. [CrossRef]

249. Yang, L.S. Novel dual DC–DC flyback converter with leakage-energy recycling. *J. Power Electron.* **2018**, *18*, 1007–1014.

250. Byen, B.J.; Jeong, B.H.; Choe, G.H. Single Pulse-Width-Modulation Strategy for Dual-Active Bridge Converters. *J. Power Electron.* **2018**, *18*, 137–146.

251. Malek, M.H.A.B.A.; Kakigano, H.; Takaba, K. Modulation strategy of dual active bridge DC–DC converter for a complete zero voltage switching operation. In Proceedings of the 2017 19th European Conference on Power Electronics and Applications (EPE'17 ECCE Europe), Warsaw, Poland, 11–14 September 2017; pp. 1–10.

252. Xiao, M.; Xu, Q.; Ouyang, H. An improved modulation strategy combining phase shifted PWM and phase disposition PWM for cascaded H-bridge inverters. *Energies* **2017**, *10*, 1327. [CrossRef]

253. Sudha, L.U.; Baskaran, J.; Elankurisil, S.A. FPGA techniques-based new hybrid modulation strategies for voltage source inverters. *Sci. World J.* **2015**. [CrossRef]

254. Lewicki, A.; Morawiec, M. Space-vector pulse width modulation for a seven-level cascaded H-bridge inverter with the control of DC-link voltages. *Bull. Pol. Acad. Sci.* **2017**, *65*, 619–625.

255. Deck, P.; Dick, C.P. Improved modulation strategy for a LLC-type resonant converter in a solar application. In Proceedings of the PCIM Europe Conference Proceedings, Nuremberg, Germany, 20–22 May 2014; pp. 1–8.

256. Dick, C.P.; Deck, P.; Schmidt, A. Optimized buck—Mode modulation strategy and control of a LLC-Type resonant converter in a solar application. In Proceedings of the 2014 16th European Conference on Power Electronics and Applications (EPE-ECCE Europe 2014), Lappeenranta, Finland, 26–28 August 2014; pp. 1–9.

257. Soubache, D.; Sivakumar, S.; Gopi Kirshna, R. A new resonant push pull converter topology for renewable sources using bidirectional switch. *Int. J. Pure Appl. Math.* **2017**, *115*, 641–646.

258. Yu, W.; York, B.; Lai, J.S. Inductorless forward-flyback soft-switching converter with dual constant on-time modulation for photovoltaic applications. In Proceedings of the 2012 IEEE Energy Conversion Congress and Exposition (ECCE 2012), Raleigh, NC, USA, 15–20 September 2012; pp. 3549–3555.

259. Taghvaee, M.H.; Radzi, M.A.M.; Moosavain, S.M.; Hizam, H.; Hamiruce Marhaban, M. A current and future study on non-isolated DC–DC converters for photovoltaic applications. *Renew. Sustain. Energy Rev.* **2013**, *17*, 216–227. [CrossRef]

260. Farahat, M.A.; Metwally, H.M.B.; Abd-Elfatah Mohamed, A. Optimal choice and design of different topologies of DC–DC converter used in PV systems, at different climatic conditions in Egypt. *Renew. Energy* **2012**, *3*, 393–402. [CrossRef]

261. Abid, R.; Masmoudi, F.; Derbel, N. Comparative study of the performances of the DC/DC luo-converter in photovoltaic applications. In Proceedings of the 2017 International Conference on Smart, Monitored and Controlled Cities (SM2C), Sfax, Tunisia, 17–19 February 2017; pp. 117–122.

262. Kasper, M.; Ritz, M.; Bortis, D.; Kolar, J.W. PV panel-integrated high step-up high efficiency isolated GaN DC–DC boost converter. In Proceedings of the 35th International Telecommunications Energy Conference (INTELEC 2013), Hamburg, Germany, 13–17 October 2013.

263. Dmitri, V.; Indrek, R. Quasi-Z-Source-Based Isolated DC/DC Converters for Distributed Power Generation. *IEEE Trans. Ind. Electron.* **2011**, *58*, 192–201.

264. Cha, H.; Peng, F.Z.; Yoo, D. Z-source resonant DC–DC converter for wide input voltage and load variation. In Proceedings of the 2010 International Power Electronics Conference (ECCE Asia, IPEC 2010), Sapporo, Japan, 21–24 June 2010; pp. 995–1000.

265. Dick, C.P.; Titiz, F.K.; De Doncker, R.W. A high-efficient LLCC series-parallel resonant converter. In Proceedings of the Conference on IEEE Applied Power Electronics Conference and Exposition (APEC), Palm Springs, CA, USA, 21–25 February 2010; pp. 696–701.

266. Liang, Z.; Guo, R.; Li, J.; Huang, A.Q. A High-Efficiency PV Module-Integrated DC/DC Converter for PV Energy Harvest in FREEDM Systems. *IEEE Trans. Power Electron.* **2011**, *26*, 897–909. [CrossRef]

267. Labella, T.; Lai, J.S. A hybrid resonant converter using a bidirectional GaN AC switch for high-efficiency PV applications. *IEEE Trans. Ind. Appl.* **2014**, *50*, 3468–3475. [CrossRef]

268. Gui, H.D.; Zhang, Z.; He, X.F.; Liu, Y.F. A high voltage-gain LLC micro-converter with high efficiency in wide input range for PV applications. In Proceedings of the Conference on IEEE Applied Power Electronics Conference and Exposition (APEC), Fort Worth, TX, USA, 16–20 March 2014; pp. 637–642.

269. Kim, Y.H.; Shin, S.C.; Lee, J.H.; Jung, Y.C.; Won, C.Y. Soft-switching current-fed push-pull converter for 250-W AC module applications. *IEEE Trans. Power Electron.* **2014**, *29*, 863–872.

270. Caracas, J.V.M.; Farias, G.D.C.; Teixeira, L.F.M.; Ribeiro, L.A.D.S. Implementation of a high-efficiency, high-lifetime, and low-cost converter for an autonomous photovoltaic water pumping system. *IEEE Trans. Ind. Appl.* **2014**, *50*, 631–641. [CrossRef]